

1 **Sources of carbonaceous aerosols and deposited black carbon in the**  
2 **Arctic in winter-spring: implications for radiative forcing**

3 Qiaoqiao Wang<sup>1</sup>, Daniel J. Jacob<sup>1</sup>, Jenny A. Fisher<sup>1</sup>, Jingqiu Mao<sup>1</sup>, Eric M.  
4 Leibensperger<sup>1</sup>, Claire C. Carouge<sup>1</sup>, Philippe Le Sager<sup>1</sup>, Yutaka Kondo<sup>2</sup>, Jose L.  
5 Jimenez<sup>3</sup>, Michael J. Cubison<sup>3</sup>, and Sarah J. Doherty<sup>4</sup>

6 <sup>1</sup> School of Engineering and Applied Sciences and Department of Earth and Planetary  
7 Sciences, Harvard University, Cambridge, Massachusetts, USA

8 <sup>2</sup> Department of Earth and Planetary Science, Graduate school of Science, University of  
9 Tokyo, Tokyo, Japan

10 <sup>3</sup> Cooperative Institute for Research in the Environmental Sciences and Department of  
11 Chemistry and Biochemistry, University of Colorado, Boulder, Colorado, USA

12 <sup>4</sup> Joint Institute for the Study of Atmosphere and Ocean, 3737 Brooklyn Ave NE, Seattle,  
13 Washington, USA

14 **Abstract**

15 We use a global chemical transport model (GEOS-Chem CTM) to interpret observations  
16 of black carbon (BC) and organic aerosol (OA) from the NASA ARCTAS aircraft  
17 campaign over the North American Arctic in April 2008, together with longer-term  
18 records in surface air and in snow. We find that Russian open fires were the dominant  
19 source of OA in the troposphere during ARCTAS but that BC was more of anthropogenic  
20 origin, particularly in surface air. This source attribution is confirmed by correlation of  
21 BC and OA with acetonitrile and sulfate in the model and in the observations. Asian  
22 emissions are the main anthropogenic source of BC in the free troposphere but European,  
23 Russian and North American sources are also important in surface air. Russian  
24 anthropogenic emissions appear to dominate the Arctic source of BC in surface air in  
25 winter. Open fire influences on Arctic surface BC in spring are much higher in the  
26 Eurasian than in the North American sector. Most of the BC transported to the Arctic in  
27 the lower troposphere is deposited within the Arctic, in contrast to the BC transported at  
28 higher altitudes. Pan-Arctic 2007-2009 observations of BC concentrations in snow are  
29 well reproduced by the model, with maximum values in the Russian Arctic and much  
30 lower values in the North American Arctic. We find that anthropogenic sources  
31 contribute 90% of BC deposited to Arctic snow in January-March and 57% in April-May  
32 2007-2009. The mean decrease in Arctic snow albedo from BC deposition is estimated to  
33 be 0.6% in spring 2007-2009, resulting in a regional surface radiative forcing consistent  
34 with previous estimates.

## 35 **1. Introduction**

36 Aerosol pollution in the Arctic peaks in winter-spring, when transport from mid-latitudes  
37 is most intense and removal by deposition is slow (Barrie et al., 1981; Quinn et al., 2002;  
38 Law and Stohl, 2007; Quinn et al., 2007). The principal submicron aerosol components  
39 are sulfate and organic aerosols (OA) (Ricard et al., 2002; Zhang et al., 2007), which  
40 affect Arctic climate by scattering solar radiation and modifying cloud properties  
41 (Kristjansson et al., 2005; Koch et al., 2007; Quinn et al., 2007; Quinn et al., 2008).  
42 Black carbon (BC) is only a minor contributor to aerosol mass but is of great climatic  
43 concern as an absorber of solar radiation both in the atmosphere (Jacobson, 2001; Koch  
44 et al., 2007; Quinn et al., 2008) and after deposition to snow (Warren and Wiscombe,  
45 1985; Flanner et al., 2007; McConnell et al., 2007; Quinn et al., 2008). Here we use a  
46 global chemical transport model (GEOS-Chem CTM) to interpret aircraft observations of  
47 BC and OA from the NASA ARCTAS campaign over the North American Arctic in  
48 April 2008 (Jacob et al., 2010), together with longer-term records of BC observations at  
49 surface sites and in snow. Our goal is to better understand the factors controlling the  
50 concentrations of carbonaceous aerosols in the Arctic, the deposition of BC to snow, and  
51 the implications for snow albedo and associated radiative forcing.

52 Historical observations of elevated BC at surface sites in the Arctic have been attributed  
53 to fossil fuel combustion in northern Europe and Russia, based on air flow back-  
54 trajectories and correlations with trace metal tracers (G. Shaw, 1982; Djupstrom et al.,  
55 1993). BC concentrations decreased from the 1980s to 2000, followed by a slight  
56 increase in the past decade (Sharma et al., 2006; Eleftheriadis et al., 2009; Gong et al.,  
57 2010; Hirdman et al., 2010). Recent measurements of BC in Arctic snow show a strong  
58 association with biomass burning based on tracer correlations and optical properties  
59 (Hegg et al., 2009; Doherty et al., 2010; Hegg et al., 2010). Stohl et al. (2007) reported an  
60 event of extremely high BC concentrations in the Arctic in spring associated with  
61 agricultural burning in Eastern Europe.

62 The origin of OA in the Arctic has received far less attention. A two-year record of OA  
63 concentrations in northern Finland shows a minimum in winter and a maximum in

64 summer attributed to biogenic and photochemical sources (Ricard et al., 2002).  
65 Measurements at Barrow show maximum OA in winter-spring, and correlations with  
66 chemical tracers suggest a dominance of ocean emissions (winter) and combustion  
67 sources (spring) (P. Shaw et al., 2010; Frossard et al., 2011).

68 Surface measurements of aerosols are not representative of the troposphere, particularly  
69 in the Arctic because of strong stratification (Klonecki et al., 2003). The vertical  
70 distribution of aerosols has important implications for radiative forcing (Koch et al.,  
71 2009a). Two coordinated aircraft campaigns with carbonaceous aerosol measurements  
72 were conducted in April 2008 out of Fairbanks, Alaska: the NASA Arctic Research of the  
73 Composition of the Troposphere from Aircraft and Satellites (ARCTAS) (Jacob et al.,  
74 2010) and the NOAA Aerosol, Radiation and Cloud Processes affecting Arctic Climate  
75 (ARCPAC) (Brock et al., 2011). These two campaigns provided extensive vertical  
76 profiling of trace gases and speciated aerosols through the depth of the Arctic troposphere.  
77 They showed in particular large enhancements of carbonaceous aerosols in the mid-  
78 troposphere due to open fires in Russia and Kazakhstan (Warneke et al., 2009; Spackman  
79 et al., 2010; Warneke et al., 2010; Kondo et al., 2011; Matsui et al., 2011; McNaughton et  
80 al., 2011).

81 A number of CTM studies have investigated the sources of BC in the Arctic, but there are  
82 large disagreements among models and discrepancies with observations (Shindell et al.,  
83 2008; Koch et al., 2009b; Tilmes et al., 2011). Emissions in East Asia have been growing  
84 and some work has pointed out an impact on winter-spring Arctic BC concentrations,  
85 especially in the free troposphere (Koch and Hansen, 2005; Shindell et al., 2008; Tilmes  
86 et al., 2011). Stohl (2006) found little wintertime Asian influence over the Arctic either at  
87 the surface or in the free troposphere. There has been far less attention to modeling OA  
88 over the Arctic, but open fires would be expected to be a dominant source (Koch et al.,  
89 2007).

90 Here we use the GEOS-Chem CTM to simulate observations of BC and OA from the  
91 DC-8 aircraft in ARCTAS, including correlations with other species, and to link the  
92 aircraft data with longer-term measurements in surface air and snow. We first evaluate  
93 the model with BC observations in northern mid-latitudes source regions to test the

94 emission inventories. We then apply the model to diagnose the sources of BC and OA in  
95 the ARCTAS aircraft data, in surface air observations, and (for BC) in 2007-2009 Arctic  
96 snow. From there we infer the radiative forcing from BC deposited to Arctic snow. This  
97 work builds on previous studies that applied GEOS-Chem to simulate observations of  
98 other species over the Arctic during ARCTAS/ARCPAC including CO (Fisher et al.,  
99 2010), sulfate-ammonium aerosols (Fisher et al., 2011), HO<sub>x</sub> radicals (Mao et al., 2010),  
100 and mercury (Holmes et al., 2010).

## 101 **2. Model description**

102 We use the GEOS-Chem CTM version 8-01-04 (<http://geos-chem.org>) driven by  
103 assimilated meteorological data from the Goddard Earth Observing System (GEOS-5) of  
104 the NASA Global Modeling and Assimilation Office (GMAO). The GEOS-5 data have  
105 6-hour temporal resolution (3-hour for surface quantities and mixing depths), 47 vertical  
106 layers, and 0.5 × 0.667 ° horizontal resolution. We degrade the horizontal resolution to  
107 2° × 2.5° for input to GEOS-Chem. We initialize the model with a one-month spin-up  
108 followed by simulation of Jan-May 2008.

109 The simulation of carbonaceous aerosols in GEOS-Chem is as described by Park et al.  
110 (2006) and Fu et al. (2009), with modifications of wet deposition and emission  
111 inventories described below. BC and primary OA (POA) are emitted by combustion.  
112 Secondary OA (SOA) is produced in the atmosphere by reversible condensation of  
113 oxidation products of biogenic and aromatic volatile organic compounds (Chung and  
114 Seinfeld, 2002; Henze and Seinfeld, 2006; Henze et al., 2008), as well as by irreversible  
115 condensation of glyoxal and methylglyoxal (Fu et al., 2008, 2009). We find that SOA  
116 formed by either of these pathways is negligible in the winter-spring Arctic and we do  
117 not discuss it further here. The simulations of BC and POA in GEOS-Chem are linear  
118 (concentrations are proportional to sources) and we isolate the contributions from  
119 different sources by tagging them in the model.

120 Dry deposition in GEOS-Chem follows a standard resistance-in-series scheme (Wesely,  
121 1989) as implemented by Wang et al. (1998). The global annual mean dry deposition  
122 velocity is 0.1 cm s<sup>-1</sup> for BC and OA, typical of current models (Reddy and Boucher,

123 2004; Huang et al., 2010a). We impose an aerosol dry deposition velocity of  $0.03 \text{ cm s}^{-1}$   
124 over snow and ice based on eddy-covariance flux measurements in the Arctic by Nilsson  
125 and Rannik (2001) and Held et al. (2011).

## 126 **2.1. Wet deposition**

127 Proper representation of scavenging by cold clouds and snow is important for simulation  
128 of aerosols in the Arctic. The standard scheme for aerosol scavenging in GEOS-Chem  
129 described by Liu et al. (2001) includes scavenging in convective updrafts, as well as in-  
130 cloud and below-cloud scavenging from convective and large-scale precipitation. Liu et  
131 al. (2001) do not distinguish between scavenging by rain and snow. Here we introduce  
132 such a distinction as well as other improvements to the scavenging scheme.

133 In the standard GEOS-Chem model, below-cloud scavenging (washout) is calculated  
134 using a washout rate constant  $S = a R$ , where  $R$  is the precipitation rate ( $\text{mm h}^{-1}$ ) and  $a =$   
135  $0.1 \text{ mm}^{-1}$  is a washout coefficient obtained by integrating scavenging efficiencies from  
136 impaction, interception, and diffusion over typical raindrop and aerosol size distributions  
137 (Dana and Hales, 1976). This overestimates integrated scavenging during a precipitation  
138 event because it does not account for the preferential removal of very fine and coarse  
139 particles, shifting the aerosol size distribution toward the more scavenging-resistant  
140 accumulation mode (Feng, 2007; Croft et al., 2009; Feng, 2009). We improve it here by  
141 using the parameterization  $S = a R^b$  constructed by Feng (2007, 2009) for individual  
142 aerosol modes (nucleation, accumulation, and coarse) and for snow as well as rain. We  
143 adopt their accumulation-mode scavenging coefficients for all aerosols except dust and  
144 sea salt, for which we adopt their coarse-mode coefficients. The corresponding values for  
145 rain ( $T \geq 268 \text{ K}$ ) are  $a = 1.1 \times 10^{-3} \text{ mm}^{-1}$  and  $b = 0.61$  for accumulation-mode aerosols, and  
146  $a = 0.92 \text{ mm}^{-1}$  and  $b = 0.79$  for coarse-mode aerosols; for snow ( $T < 268 \text{ K}$ ), they are  $a =$   
147  $2.8 \times 10^{-2} \text{ mm}^{-1}$  and  $b = 0.96$  for accumulation-mode aerosols, and  $a = 1.57 \text{ mm}^{-1}$  and  $b =$   
148  $0.96$  for coarse-mode aerosols. Scavenging of accumulation-mode aerosols by snow is an  
149 order of magnitude more efficient than by rain because of the larger areal cross section of  
150 snow crystals (Murakami et al., 1983).

151 In-cloud scavenging (rainout) efficiently removes aerosols serving as cloud condensation  
 152 nuclei (CCN) or ice nuclei (IN). In the case of warm and mixed-phase clouds ( $T > 258$  K),  
 153 we assume 100% incorporation of hydrophilic aerosols in the cloud droplets followed by  
 154 efficient scavenging when liquid water is converted to precipitation by coalescence or  
 155 riming. We assume that 80% of BC and 50% of POA are emitted as hydrophobic (Cooke  
 156 et al., 1999; Park et al., 2003), and convert them to hydrophilic in the atmosphere with an  
 157 e-folding time of 1 day which yields a good simulation of BC export efficiency in  
 158 continental outflow (Park et al., 2005). In the case of cold clouds ( $T < 258$ K), we assume  
 159 that only dust and hydrophobic BC can serve as IN and hence be removed by scavenging  
 160 (Chen et al., 1998; Andreae and Rosenfeld, 2008), with the acknowledgment that cold-  
 161 cloud aerosol scavenging is highly uncertain (Karcher et al., 2007; Baumgardner et al.,  
 162 2008; Cozic et al., 2008; Targino et al., 2009).

163 Precipitation is a subgrid process on the horizontal scale of GEOS-Chem. A critical  
 164 variable in the wet deposition parameterization is the areal fraction  $F_k$  of a grid box at  
 165 vertical model layer  $k$  that actually experiences precipitation. Liu et al. (2001) applied the  
 166 formulation of Giorgi and Chameides (1986) for the areal fraction  $F'_k$  over which new  
 167 precipitation is formed:

$$168 \quad F'_k = \frac{Q_k}{LC_1} \quad (1)$$

169 where  $Q_k$  is the grid-scale formation rate of new precipitation ( $\text{kg m}^{-3} \text{s}^{-1}$ ),  $L$  is the  
 170 condensed water content of the precipitating cloud and is assumed to be constant ( $L =$   
 171  $1.0 \times 10^{-3} \text{ kg m}^{-3}$ ) (DelGenio et al., 1996), and  $C_1$  is the rate constant for conversion of  
 172 cloud water to precipitation ( $C_1 = C_{1min} + Q_k / L$  with  $C_{1min} = 1.0 \times 10^{-4} \text{ s}^{-1}$ ). The algorithm  
 173 is initiated for each grid square at the top of the tropospheric column and proceeds  
 174 downward, computing the actual precipitating fraction  $F_k$  in layer  $k$  (index decreasing  
 175 downward) as  $F_k = \max(F'_k, F_{k+1})$  to account for precipitation formation overhead. In  
 176 previous versions of GEOS-Chem,  $Q_k > 0$  caused rainout to be applied to the whole  
 177 precipitation area fraction  $F_k$  and washout was only applied when  $F_k > 0$  and  $Q_k \leq 0$   
 178 (negative  $Q_k$  indicating net evaporation). This caused an overestimation of in-cloud  
 179 scavenging and underestimation of below-cloud scavenging, as  $F_{k+1} > F'_k$  should be an

180 indication of washout taking place over the fractional area  $F_{k+1} - F'_k$  of layer  $k$ . In our  
181 present simulation, we apply rainout in layer  $k$  to the precipitating fraction  $F'_k$  and  
182 washout to the additional fractional area  $F_{diff} = \max(0, F_{k+1} - F'_k)$ . The correction slows  
183 aerosol scavenging as washout is generally less efficient than rainout. The global lifetime  
184 of carbonaceous aerosols in our simulation is 6 days, within the range of 5-11 days from  
185 current models (Koch et al., 2009b).

186 Model transport of BC from northern mid-latitudes to the Arctic is highly sensitive to  
187 assumptions about scavenging efficiency. Liu et al. (2011) found in their AM-3 model a  
188 factor of 100 increase in winter-spring Arctic BC, and better agreement with observations  
189 from surface sites and from ARCTAS, by using a photochemically-varying timescale for  
190 BC hydrophobic-to-hydrophilic aging (up to 1-2 weeks in winter) and reducing  
191 deposition efficiencies relative to their original model. They found in their model that 30-  
192 50% of Arctic BC remained hydrophobic in winter. However, TRACE-P aircraft  
193 observations in Asian outflow in March-April provide good constraints that the BC aging  
194 time scale is no more than 2 days (Park et al., 2005), and aircraft observations of light  
195 absorption in ARCTAS implied significant coating for the BC particles (McNaughton et  
196 al., 2011).

## 197 **2.2. Emissions of BC and OA**

198 Figure 1 shows the hemispheric emissions of BC and POA (primary organic aerosol) in  
199 April 2008 in the model. Table 1 gives regional and global annual totals for 2008. The  
200 source regions are chosen to encompass the bulk of Northern Hemisphere emissions.  
201 Anthropogenic emissions (fossil fuel and biofuel combustion) are from Bond et al. (2007)  
202 for 2000, but with doubled emissions in Russia and Asia (including China, India, Korea  
203 and Japan) for both BC and POA to match BC surface observations in China and in the  
204 Arctic as discussed below. This doubling would be consistent with the strong recovery of  
205 the Russian economy since 2000 (IEA, 2010) and with the general increase in Chinese  
206 emissions over the past decade (Zhang et al., 2008a; Lu et al., 2010).

207 April 2008 saw exceptionally high forest and agricultural fire activity in Russia and  
208 Kazakhstan (hereafter referred to collectively as “Russia”) (Warneke et al., 2009; Fisher

209 et al., 2010) as well as typical seasonal fire activity in Southeast Asia (including India  
210 and southern China). We specify open fire emissions with the Fire Locating and  
211 Monitoring of Burning Emissions (FLAMBE) inventory (Reid et al., 2009), which has  
212  $1^\circ \times 1^\circ$  spatial resolution and hourly temporal resolution based on MODIS and GOES  
213 satellite fire counts. The FLAMBE inventory provides fine particle ( $PM_{2.5}$ ) emissions  
214 based on total estimated fuel combustion, carbon fraction in the fuel, and  $PM_{2.5}$  emission  
215 factors (Reid et al., 2005, 2009). We partition  $PM_{2.5}$  emissions into BC and OA using  
216 emission factors from Andreae and Merlet (2001) for different vegetation types. Fisher et  
217 al. (2010) previously used FLAMBE to simulate ARCTAS/ARCPAC CO observations  
218 with GEOS-Chem and found that Russian and Southeast Asian emissions needed to be  
219 reduced to 53% and 45%, respectively. We apply here the same reductions to BC and OA  
220 emissions. Open fires in Russia were the dominant source of OA in ARCTAS (Warneke  
221 et al., 2009, 2010), and we find from tagged source attribution that OA emissions from  
222 Russian fires must be reduced by an additional 36% to match the ARCTAS observations.  
223 This defines our OA emission factor from the fires, given below.

224 To define the BC emission factor from the Russian fires we use observations of the  
225 BC/OA concentration ratio in fire plumes. Warneke et al. (2009) reported BC/OA ratios  
226 of 0.14 (agricultural fires) and 0.15 (forest fires) on a carbon basis for Russian fire  
227 plumes sampled in ARCPAC, and we find a similar observed ratio of  $0.12 \pm 0.03$  for fire  
228 plumes sampled in ARCTAS (Figure 2). A BC/OA emission ratio in the model of 0.13  
229 from fires reproduces these values in the fire plumes. The resulting emission factors for  
230 Russian fires used in the model are  $0.87 \text{ g kg}^{-1}$  (gram carbon per kilogram dry mass  
231 burned) for BC and  $6.8 \text{ g kg}^{-1}$  for OA, consistent with the values of 0.30-0.82 and 2.0-9.7  
232 reported in the literature (Andreae and Merlet, 2001; Akagi et al., 2011).

233 Figure 3 compares annual mean surface air concentrations of BC in the model in 2008  
234 with observations from networks in the US (2008), China (2006), and Europe (2002-  
235 2003). Our objective is to diagnose any large model bias in these three major source  
236 regions relevant to the Arctic. For the US we use 2008 data from the rural IMPROVE  
237 network (<http://vista.cira.colostate.edu/improve/Data/IMPROVE/AsciiData.-aspx>). For  
238 China and Europe we do not have network observations for 2008, and use therefore data

239 for other years with the assumption that interannual variability is small: Zhang et al.  
240 (2008b) for rural/regional sites in China in 2006, and the BC/OC campaign in Europe in  
241 2002-2003 (<http://tarantula.nilu.no/projects/ccc/-emepdata.html>). We diagnose for each  
242 region the normalized mean bias:

$$243 \quad NMB = 100\% \times \sum_i (M_i - O_i) / \sum_i O_i \quad (2)$$

244 where the sum is over the ensemble of sites  $i$ , and  $M_i$  and  $O_i$  are the modeled and  
245 observed values, respectively.

246 The data in Figure 3 show normalized mean biases of -24% for China, -31% for Europe,  
247 and +35% for the US. Without doubling the inventory from Bond et al. (2007) the bias  
248 for China would be much larger (NMB = -61%). Underestimation in Europe is mainly  
249 due to three sites in northern Italy and Belgium. Without these three sites the NMB would  
250 decrease to -0.7%. The overestimation of BC in the US can be explained by a 40%  
251 decrease in observed concentrations between 2000 (year of the Bond et al. (2007)  
252 inventory) and 2008, as shown by Leibensperger et al. (2011).

### 253 **3. Sources of BC and OA in the Arctic**

#### 254 **3.1. Constraints from aircraft data**

255 Figure 4 shows the DC-8 flight tracks in ARCTAS. BC was measured with a SP2 (Single  
256 Particle Soot Photometer) instrument (Kondo et al., 2011). OA and other aerosol  
257 information were measured by an Aerosol Mass Spectrometer (AMS) (Jimenez et al.,  
258 2003) for sub-micrometer particles, which we assume account for the bulk of OA. The  
259 AMS measures OA in units of  $\mu\text{g m}^{-3}$  and we convert this to  $\mu\text{g C m}^{-3}$  with a ratio of 2.1  
260 typical of nonurban aerosols (Turpin and Lim, 2001; Aiken et al., 2008). The model is  
261 sampled along the flight tracks at the same time and location as the observations, and the  
262 aircraft data are averaged over the GEOS-Chem grid. Observations outside the Arctic  
263 (south of  $60^\circ\text{N}$ ), in the stratosphere ( $[\text{O}_3]/[\text{CO}] > 1.25 \text{ mol mol}^{-1}$ ), and in fire plumes  
264 ( $[\text{CH}_3\text{CN}] > 200 \text{ ppt}$ ) are excluded. We previously used the information from fire plumes  
265 to constrain the BC emission factor (Section 2).

266 BC and OA were measured from the ARCPAC aircraft concurrently with ARCTAS, but  
267 for fewer flights and a much smaller spatial domain around Fairbanks. Fisher et al. (2011)  
268 previously compared the GEOS-Chem sulfate-ammonium aerosol simulation to the  
269 ensemble of ARCTAS and ARCPAC observations, and found the ARCPAC data difficult  
270 to interpret because of the limited sampling and focus on fire plumes. We limit here our  
271 use of the ARCPAC data to the constraints that they provide on biomass burning  
272 emission factors (Warneke et al., 2009, 2010) and BC deposition (Spackman et al., 2010).

273 Figure 5 shows the overall fine aerosol composition measured by the ARCTAS DC-8 in  
274 2-km altitude bins, providing context for the relative importance of BC and OA. Sea salt  
275 and dust are excluded as only bulk measurements were made in ARCTAS and we expect  
276 their coarse-mode fractions to be dominant. OA and sulfate are the dominant components  
277 of the fine aerosol. Sulfate is dominant in surface air but OA becomes comparable in the  
278 free troposphere, because sulfate shows little variation with altitude while OA is strongly  
279 peaked at 2-6 km.

280 Figure 6 shows scatterplots of simulated vs. observed BC and OA concentrations during  
281 ARCTAS, and Figure 7 shows mean vertical profiles. The model has some success in  
282 reproducing the variability of the individual observations, with a correlation coefficient  $r$   
283 = 0.65 for BC and 0.62 for OA. There are some large underestimates in the mid-  
284 troposphere associated with elevated  $\text{CH}_3\text{CN}$ , a tracer of biomass burning, but these may  
285 reflect the inability of the model to resolve fine plumes not screened by the  $[\text{CH}_3\text{CN}] <$   
286 200 ppt filter. Eulerian models such as GEOS-Chem cannot resolve fine structures  
287 (Rastigejev et al., 2010). Concentrations of BC average  $53 \pm 109 \text{ ng C m}^{-3}$  in the  
288 observations and  $63 \pm 65 \text{ ng C m}^{-3}$  in the model. Concentrations of OA average  $0.40 \pm 0.56$   
289  $\mu\text{g C m}^{-3}$  in the observations and  $0.35 \pm 0.37 \mu\text{g C m}^{-3}$  in the model.

290 The model successfully reproduces the mean vertical distributions of BC and OA, with  
291 peaks in the mid-troposphere. Model source attribution in Figure 7 shows that these peaks  
292 are due to Russian fires, and in the case of BC also to Asian anthropogenic influence.  
293 Fires contribute 46% of BC and 84% of OA at 2-6 km altitude in the model. The mid-  
294 tropospheric maximum reflects the lifting of Russian fire and Asian pollution effluents by  
295 warm conveyor belts (WCBs) originating from the Pacific Rim of the Asian continent

296 (Liu et al., 2003; Stohl, 2006; Fisher et al., 2010). The strong influence of open fires at 2-  
297 6 km is consistent with the observed strong correlations of BC vs. CH<sub>3</sub>CN ( $r=0.74$ ) and  
298 OA vs. CH<sub>3</sub>CN ( $r=0.81$ ) and has been reported in previous ARCTAS/ARCPAC analyses  
299 (Warneke et al., 2009; Spackman et al., 2010; Warneke et al., 2010; Kondo et al., 2011;  
300 Matsui et al., 2011).

301 We find that open fires are the dominant source of OA at all altitudes in the model, but  
302 anthropogenic sources are more important for BC and completely dominate near the  
303 surface (Figure 7). We evaluate this source attribution by using observed and simulated  
304 correlations with sulfate, an aerosol tracer of anthropogenic influence. Simulated GEOS-  
305 Chem sulfate is from Fisher et al. (2011). Figure 8 shows observed and simulated  
306 scatterplots of BC and OA vs. sulfate, indicating good agreement in the correlation  
307 coefficients and the slopes of the regression lines at 2-6 km (mid-troposphere) and 0-1  
308 km (near-surface). There is significant correlation between OA and sulfate in the mid-  
309 troposphere, consistent with the well-known mixing of pollution and fire influences in  
310 Asian outflow lifted by WCBs (Bey et al., 2001) and previously documented in ARCTAS  
311 and ARCPAC (Fisher et al., 2010; Brock et al., 2011). Figure 8 shows a population of  
312 points at altitude > 6 km with extremely high sulfate concentrations (> 3  $\mu\text{g m}^{-3}$  STP) and  
313 low BC and OA concentrations, corresponding to a plume transported from East Asia as  
314 indicated by back-trajectories. The strong enrichment of sulfate relative to carbonaceous  
315 aerosols in that plume is consistent with Asian pollution having experienced wet  
316 scavenging, as previously shown by van Donkelaar et al. (2008) and Dunlea et al. (2009)  
317 in observations from the INTEX-B aircraft campaign.

318 The contribution of open fire emissions in the model decreases from the mid-troposphere  
319 to near-surface air (<1 km), where it accounts for 20% of BC and 60% of OA. The  
320 concentration ratios relative to sulfate are also much lower in near-surface air than in the  
321 mid-troposphere, both in the model and in observations (Figure 8). This is consistent with  
322 Fisher et al. (2011), who found a major contribution to Arctic boundary layer sulfate from  
323 boundary layer transport of European and North American pollution, in contrast to the  
324 mid-troposphere where Asian pollution dominates. This boundary layer anthropogenic  
325 influence, adding to the subsidence from the mid-troposphere, is far more important for

326 BC than for OA because of the much higher BC/OA emission ratio from anthropogenic  
327 sources than from open fires (Table 1). Consequently, the observed ratio of BC vs. OA  
328 increases from 0.17 in the mid-troposphere to 0.26 near the surface (Figure 9), and this is  
329 also well captured in the model.

330 Our estimation of the open fire contribution to BC along the ARCTAS DC-8 flight tracks  
331 agrees with the value of 33-41% reported by McNaughton et al. (2011) using CH<sub>3</sub>CN and  
332 the OA/sulfate ratio to classify the data. Matsui et al. (2011) attributed most of the BC  
333 measured in ARCTAS to Russian fire emissions using CH<sub>3</sub>CN and dichloromethane  
334 (CH<sub>2</sub>Cl<sub>2</sub>) to classify the data, but their analysis focused on plumes and ignored  
335 background air.

336 Broader examination of model results over the scale of the Arctic polar cap (north of  
337 60°N) in April 2008 indicates that open fire emissions contribute 50% of total BC in the  
338 Arctic tropospheric column and 81% of total OA. Fire influences are the strongest in the  
339 Eurasian Arctic (not sampled by the aircraft). Asian pollution dominates the source of  
340 anthropogenic BC in the Arctic tropospheric column, but less so in surface air which is  
341 most relevant for BC deposition to snow (Shindell et al., 2008; Huang et al., 2010b). Our  
342 model Asian contribution to Arctic BC in spring is higher than previous studies (Koch  
343 and Hansen, 2005; Shindell et al., 2008; Tilmes et al., 2011). This reflects our higher  
344 Asian emission inventory, constrained by observations at Chinese sites as discussed in  
345 Section 2.

### 346 **3.2. Surface observations**

347 We now turn to surface observations in Jan-May 2008 to provide broader seasonal  
348 context. Figure 10 compares model results with monthly average surface concentrations  
349 observed in Alaska at Denali (low Arctic) and Barrow (high Arctic) in 2002-2008  
350 (locations shown in Figure 4). Model contributions from different sources are shown.  
351 Observations at Denali are from the IMPROVE network (<http://vista.cira.colostate.edu/improve/Data/IMPROVE/AsciiData.aspx>) using a thermal/optical reflectance method.  
352 Observations at Barrow are from the NOAA Global Monitoring Division  
353 (<http://www.esrl.noaa.gov/gmd/aero/net/>), reported as aerosol light absorption  
354 coefficients from a particle soot absorption photometer. We use a mass absorption  
355

356 efficiency of  $9.5 \text{ m}^2 \text{ g}^{-1}$  to convert the absorption coefficients to BC mass concentrations  
357 based on ARCTAS data (McNaughton et al., 2011). OA observations at Barrow are from  
358 P. Shaw et al. (2010), who reported seasonal mean concentrations for Mar 2008-Mar  
359 2009.

360 We find that the BC and OA observations at the surface sites in April 2008 are roughly  
361 consistent with the mean near-surface ARCTAS data (Figure 7), but are more affected by  
362 Russian fires. The fire influence at Denali is larger than that at Barrow. Observations in  
363 April 2008 were anomalously high relative to the 2002-2008 April mean (thin lines in  
364 Figure 9), which reflects the anomalously large Russian fires (Fisher et al., 2010).

365 Observations of BC at Barrow show higher values in winter (Jan-Mar) than spring (Apr-  
366 May), even in 2008. In contrast, Denali shows higher values in spring even in the 2002-  
367 2008 mean. The model fails to reproduce the seasonal variation at Denali, apparently  
368 because it overestimates local pollution influence from nearby Anchorage in winter. It is  
369 more successful at Barrow, although this is contingent on doubling of the Russian  
370 anthropogenic source from the Bond et al. (2007) inventory as described above. The  
371 winter maximum at Barrow is explained in the model by the Russian anthropogenic  
372 source, transported to the North American Arctic in the boundary layer around the  
373 Siberian High with little dilution and little precipitation. This Russian source influence  
374 declines sharply in spring due to vertical mixing and to the weakening of the Siberian  
375 High. Sharma et al. (2006) found similar source attribution for BC at Barrow using back-  
376 trajectory analysis, and Fisher et al. (2011) found similar results for sulfate at Barrow  
377 using GEOS-Chem.

378 Observed OA at Denali shows similar winter-spring seasonality as BC. Our model  
379 reproduces this seasonality without the spurious local influence from Anchorage seen for  
380 BC (the OA/BC emission ratio from Anchorage in the Bond et al. (2007) inventory is 50%  
381 lower than the anthropogenic mean). Observations of OA at Barrow show little seasonal  
382 variation between winter and spring, which is consistent with the model as the decline in  
383 the Russian anthropogenic source from winter to spring is compensated by the open fire  
384 influence. Both at Denali and at Barrow, we find that we can largely explain the  
385 wintertime OA on the basis of anthropogenic sources and the springtime OA on the basis

386 of open fires. The source attribution in spring is consistent with the work of P. Shaw et al.  
387 (2010) and Frossard et al. (2011), who identified a dominant combustion source for OA  
388 at Barrow on the basis of correlations with combustion tracers. But P. Shaw et al. (2010)  
389 also attributed most OA at Barrow in winter to oceanic emissions, which are not included  
390 here.

#### 391 **4. BC deposition in the Arctic and implications for radiative forcing**

392 BC transported to the Arctic can either be removed by deposition or eventually ventilated  
393 out. We find in model sensitivity simulations that BC transported to the Arctic below 2  
394 km is mostly deposited within the Arctic, whereas BC transported to the Arctic at higher  
395 altitudes is mostly ventilated out. Deposition is mainly by wet processes (90%).  
396 Spackman et al. (2010) inferred a dry deposition flux for BC of 170-1700 ng m<sup>-2</sup> day<sup>-1</sup>  
397 over snow/ice during ARCPAC on the basis of observed BC depletion in the boundary  
398 layer. Our computed dry deposition flux in the Western Arctic (mostly covered by  
399 snow/ice) is about 1500 ng m<sup>-2</sup> day<sup>-1</sup> in spring, consistent with that estimate.

400 Figure 11 shows the spatial distribution of model BC deposition in winter (Jan-Mar) and  
401 spring (Apr-May) 2008, separately for open fire and anthropogenic contributions.  
402 Maximum deposition is in the Eurasian sector due to Russian and European  
403 anthropogenic sources, augmented in spring by Russian fires. The fires double BC  
404 deposition to the Arctic in spring relative to winter. The Asian anthropogenic  
405 contribution to BC deposition is very small in winter compared to European and Russian  
406 sources but becomes comparable to these sources in the spring.

407 While ARCTAS data only provide information for the North American Arctic, we find  
408 that the largest BC deposition flux to the Arctic is in the Eurasian sector with a dominant  
409 contribution from open fires during spring 2008 (Figure 11). Doherty et al. (2010)  
410 reported snow BC concentrations from a large network of both Russian and North  
411 American Arctic sites in Mar-May 2007-2009. We compared these observations  
412 (available for download at <http://www.atmos.washington.edu/sootinsnow/>) to model  
413 values for the corresponding years, using the GFEDv2 fire inventory for 2007 (van der  
414 Werf et al., 2006) and the FLAMBE inventory with above scaling factors for 2009.

415 MODIS fire counts show that spring 2007 had lower-than-average Russian fires while  
416 2009 was near average, offering a contrast to spring 2008 which had anomalously high  
417 Russian fire activity (Fisher et al. (2010); <http://disc.sci.gsfc.nasa.gov/giovanni/>). The  
418 total model BC deposition to the Arctic in April-May is 16 Gg month<sup>-1</sup> for 2007  
419 (including 13% from open fires), 41 Gg month<sup>-1</sup> for 2008 (61%), and 34 Gg month<sup>-1</sup> for  
420 2009 (46%). Deposition in Jan-Mar has little interannual variability (14-19 Gg month<sup>-1</sup>).

421 Figure 12 shows model results for the BC content of snow in winter (Jan-Mar) and spring  
422 (Apr-May) 2007-2009, as calculated from the ratio of BC to water deposition fluxes. The  
423 Doherty et al. (2010) sampling locations are indicated by purple circles. Model values are  
424 much higher over the Eurasian than the North American Arctic. There is relatively little  
425 variability over the Arctic Ocean. Low values over Greenland reflect the elevated surface.  
426 The mean BC snow content over the scale of the Arctic shows only weak interannual  
427 variability in winter (12-15 ng g<sup>-1</sup>) but large interannual variability in spring (13-38 ng g<sup>-1</sup>)  
428 <sup>1</sup>), reflecting the open fire influence as discussed above.

429 Figure 13 shows scatterplots of simulated vs. observed BC content in snow for the  
430 Doherty et al. (2010) sites in the North American and Russian Arctic sectors.  
431 Observations are averaged over the model grid squares and the model is sampled for the  
432 month and year of observations. Model and observations in the North American Arctic  
433 sector generally agree within a factor of 2. Excluding the outlier with observed value of  
434 30 ng g<sup>-1</sup> in 2007, we find a good correlation between observations and the model with  
435  $r=0.60$ . Mean values are  $11\pm 4$  ng g<sup>-1</sup> in the observations and  $11\pm 3$  ng g<sup>-1</sup> in the model.  
436 Rough agreement between model and observations is also found in the Russian Arctic  
437 sector, with mean values of  $31\pm 11$  ng g<sup>-1</sup> in the model and  $23\pm 16$  ng g<sup>-1</sup> in the  
438 observations. The model indicates a dominant anthropogenic influence over western  
439 Russia in 2007 and a dominant open fire influence over eastern Russia in 2008, consistent  
440 with the analysis by Doherty et al. (2010).

441 Model source attribution shows that the mean contribution of open fires to the BC content  
442 in Arctic snow is 10% in winter and 65% in spring 2008 (43% for springs 2007-2009). It  
443 is dominant in the Russian Arctic sector in spring 2008 and in the western Russian Arctic  
444 sector in spring 2009. Hegg et al. (2009, 2010) and Doherty et al. (2010) previously

445 reported a dominant influence from biomass burning in their BC snow content data,  
446 based on absorption Ångström exponents and correlation with biomass burning tracers.  
447 Part of the discrepancy could reflect biofuel combustion, which accounts in the model for  
448 38% of annual anthropogenic emissions in Asia and 25% in Russia, and would be highest  
449 in winter-spring due to residential heating. In addition, mixing of anthropogenic and fire  
450 influences in Asian outflow discussed above complicates source attribution in the  
451 observations; this mixing is apparent in the Hegg et al. (2010) analysis as an association  
452 of sulfate with biomass burning influence.

453 Figure 14 shows model results for the decreases in snow albedo in winter (Jan-Mar) and  
454 spring (Apr-May) 2008 due to BC deposition to snow. We assume a constant snow grain  
455 radius of 100 $\mu\text{m}$  (McConnell et al., 2007) with no significant aging, and estimate the  
456 effect of BC on snow albedo based on Figure 2 in Warren and Wiscombe (1995). The  
457 resulting decrease in snow albedo averaged over the Arctic is 0.4% in winter and 0.8% in  
458 spring 2008 (0.6% for spring 2007-2009), lower than previous estimates of 1.1-4.7%  
459 (Park et al., 2005; Flanner et al., 2007; Koch et al., 2009a). By convolving this result with  
460 the GEOS-5 incoming solar radiation at the surface we deduce a radiative forcing over  
461 the Arctic (north of 60°N) from deposited BC of 0.1  $\text{W m}^{-2}$  in winter and 1.7  $\text{W m}^{-2}$  in  
462 spring 2008 (1.2  $\text{W m}^{-2}$  for spring 2007-2009, including 0.6  $\text{W m}^{-2}$  from anthropogenic  
463 sources only). A previous model calculation by Flanner et al. (2007) reported a radiative  
464 forcing of 0.02  $\text{W m}^{-2}$  in winter and 0.53  $\text{W m}^{-2}$  in spring due to anthropogenic BC over  
465 the same domain, similar to our values. The global annual mean radiative forcing due to  
466 the snow-albedo effect from anthropogenic BC is 0.13  $\text{W m}^{-2}$  in our simulation, with a  
467 maximum in China (similar to the distribution described in Flanner et al. (2007)). This is  
468 within the range estimated by the IPCC (0.1  $\pm$  0.1  $\text{W m}^{-2}$ ) (Forster et al., 2007).

## 469 **5. Conclusions**

470 We used the GEOS-Chem chemical transport model (CTM) to interpret aircraft  
471 observations of black carbon (BC) and organic aerosol (OA) from the NASA ARCTAS  
472 campaign over the North American Arctic in April 2008, together with longer-term  
473 observations of BC concentrations in surface air and 2007-2009 pan-Arctic observations

474 of BC snow content. Our focus was to quantify the contributions of different source types  
475 and source regions to Arctic BC and OA concentrations in winter-spring, the role of  
476 deposition processes, the resulting source attribution for BC in snow, and the implications  
477 for radiative forcing.

478 Our GEOS-Chem simulation includes an improved representation of aerosol scavenging  
479 by cold clouds and by snow, anthropogenic emissions of BC and OA from the Bond et al.  
480 (2007) inventory for 2000, and open fire emissions from the FLAMBE inventory of Reid  
481 et al. (2009) with hourly resolution. We evaluated BC sources from the northern mid-  
482 latitude continents with data from observation networks. We find that Russian and Asian  
483 anthropogenic emissions have to be doubled from Bond et al. (2007) to improve the  
484 match to observations for BC, as might be expected from increasing fuel use in these  
485 regions since 2000. Unusually large fires occurred in Russia in April 2008. FLAMBE  
486 estimates of biomass burned for these fires had to be decreased as previously shown by  
487 Fisher et al. (2010) from ARCTAS and satellite CO data. We find that BC and OA fire  
488 emission factors of 0.87 and 6.8 g carbon per kg dry mass burned, respectively, give a  
489 good simulation of observed Russian fire plumes.

490 The resulting model provides a good fit to the mean observed concentrations and vertical  
491 gradients of BC and OA along the ARCTAS flight tracks. Open fires account for most of  
492 OA in the model while anthropogenic emissions are more important for BC. Model and  
493 observations show strong peaks in the mid-troposphere for both BC and OA, reflecting  
494 the transport of Russian fire and Asian anthropogenic effluents lifted by warm conveyor  
495 belts (WCBs). Open fires contribute 46% of BC and 84% of OA in the mid-troposphere  
496 (2-6 km) in the model. Near the surface (<1 km), by contrast, we find that fires contribute  
497 only 20% of BC and 60% of OA. Anthropogenic BC concentrations in the mid-  
498 troposphere are mostly of Asian anthropogenic origin, but in surface air we find  
499 comparable contributions from North America and Europe. These model source  
500 attributions are consistent with observed correlations of BC and OA with acetonitrile (a  
501 tracer of biomass burning) and with comparisons of simulated and observed correlations  
502 of BC and OA vs. sulfate. The dominant influence of open fire emissions on OA agrees  
503 with the previous work of Warneke et al. (2009, 2010). The much smaller contribution

504 from open fires to ARCTAS BC is consistent with the previous work of McNaughton et  
505 al. (2011) but not with that of Warneke et al. (2010) and Matsui et al. (2011) who we  
506 argue gave excessive consideration to fire plumes.

507 Expanding the model results to the scale of the Arctic polar cap in April 2008 indicates  
508 that open fire emissions contribute 50% of total BC in the Arctic tropospheric column  
509 and 81% of total OA. We find the strongest fire influences in the Eurasian Arctic, with  
510 the highest BC and OA concentrations there. Asian pollution dominates the source of  
511 anthropogenic BC in the Arctic tropospheric column, but less so in surface air which is  
512 most relevant for BC deposition to snow (Shindell et al., 2008; Huang et al., 2010b). Our  
513 relatively higher model Asian contribution to Arctic BC in spring compared with  
514 previous studies (Koch and Hansen, 2005; Shindell et al., 2008; Tilmes et al., 2011)  
515 reflects our higher Asian emission inventory, constrained by observations at Chinese sites.

516 We used surface air observations of BC and OA at two Alaskan sites (Denali and Barrow)  
517 in Jan-May 2002-2008 to place the aircraft data in a seasonal context. BC concentrations  
518 and model source attributions for April 2008 are consistent between the surface sites and  
519 the aircraft. The Denali site shows an increase of BC from winter to spring due to  
520 Russian fire and Asian pollution influences. The seasonality is reversed at Barrow with a  
521 winter maximum that we attribute to transport from Russia. A similar seasonal transition  
522 in source influence on BC at Barrow has been reported by Sharma et al. (2006) based on  
523 back-trajectory analyses. OA concentrations at Denali and Barrow are well simulated by  
524 the model, with similar sources as for BC, but with stronger impact of fire emissions in  
525 spring that dampens the seasonality at Barrow.

526 Spring 2008 was anomalously affected by Russian fires. We conducted simulations for  
527 Jan-May 2007-2009 to obtain an interannual perspective on BC deposition to the Arctic  
528 and to evaluate the model with a pan-Arctic network of observations of BC snow content  
529 (Doherty et al., 2010). We find in the model that the total BC deposition flux to the Arctic  
530 in 2007-2009 averages 17 (14-19) Gg month<sup>-1</sup> in Jan-Mar and 30 (16-41) Gg month<sup>-1</sup> in  
531 Apr-May, where the range indicates the interannual variability. Open fires contribute  
532 much more to BC deposition in the Eurasian Arctic than in the North American Arctic.  
533 The model reproduces well the observations of BC snow content and their variability,

534 with highest values in the Russian Arctic and lowest in Greenland. In the model,  
535 anthropogenic sources account on average for 10% of BC content in the Arctic snow in  
536 Jan-Mar and 43% in Apr-May 2007-2009. Hegg et al. (2009, 2010) and Doherty et al.  
537 (2010) previously found a dominant biomass burning influence at most of their Arctic  
538 sites on the basis of correlations with tracers and absorption Ångstrom exponents. Some  
539 of that influence could reflect biofuel use (38% of annual BC anthropogenic emissions in  
540 Asia according to Bond et al. (2007)). Mixing of anthropogenic and fire influences also  
541 complicates source attribution in the observations.

542 We estimate decreases in snow albedo due to BC deposition in 2007-2009 to be 0.4% in  
543 winter and 0.6% in spring. The resulting mean surface radiative forcing over the Arctic in  
544 spring is  $1.2 \text{ W m}^{-2}$  (including open fires) and  $0.6 \text{ W m}^{-2}$  (anthropogenic only). This is  
545 consistent with the anthropogenic value of  $0.53 \text{ W m}^{-2}$  previously reported by Flanner et  
546 al. (2007) for the same region. Averaged over the global scale, we find an annual mean  
547 surface radiative forcing of  $0.13 \text{ W m}^{-2}$  from BC deposited to snow, within the range  
548 reported in IPCC 2007 (Forster et al., 2007).

549 **Acknowledgments.** This work was funded by the Decadal and Regional Climate  
550 Prediction using Earth System Models (EaSM) Program of the US National Science  
551 Foundation. MJC and JLJ were supported by NASA grant NNX08AD39G.

552 **References:**

- 553 Aiken, A. C., DeCarlo, P. F., Kroll, J. H., Worsnop, D. R., Huffman, J. A., Docherty, K.  
554 S., Ulbrich, I. M., Mohr, C., Kimmel, J. R., Sueper, D., Sun, Y., Zhang, Q., Trimborn, A.,  
555 Northway, M., Ziemann, P. J., Canagaratna, M. R., Onasch, T. B., Alfarra, M. R., Prevot,  
556 A. S. H., Dommen, J., Duplissy, J., Metzger, A., Baltensperger, U., and Jimenez, J. L.:  
557 O/C and OM/OC ratios of primary, secondary, and ambient organic aerosols with high-  
558 resolution time-of-flight aerosol mass spectrometry, *Environ. Sci. Technol.*, 42, 4478-  
559 4485, doi:10.1021/es703009q, 2008.
- 560 Akagi, S. K., Yokelson, R. J., Wiedinmyer, C., Alvarado, M. J., Reid, J. S., Karl, T.,  
561 Crounse, J. D., and Wennberg, P. O.: Emission factors for open and domestic biomass  
562 burning for use in atmospheric models, *Atmos. Chem. Phys.*, 11, 4039-4072,  
563 doi:10.5194/acp-11-4039-2011, 2011.
- 564 Andreae, M. O., and Merlet, P.: Emission of trace gases and aerosols from biomass  
565 burning, *Glob. Biogeochem. Cycle*, 15, 955-966, 2001.
- 566 Andreae, M. O., and Rosenfeld, D.: Aerosol-cloud-precipitation interactions. Part 1. The  
567 nature and sources of cloud-active aerosols, *Earth-Sci. Rev.*, 89, 13-41,  
568 doi:10.1016/j.earscirev.2008.03.001, 2008
- 569 Barrie, L. A., Hoff, R. M., and Daggupaty, S. M.: The influence of mid-latitude  
570 pollution sources on haze in the Canadian Arctic, *Atmos. Environ.*, 15, 1407-1419, 1981.
- 571 Baumgardner, D., Subramanian, R., Twohy, C., Stith, J., and Kok, G.: Scavenging of  
572 black carbon by ice crystals over the northern Pacific, *Geophys. Res. Lett.*, 35, L22815,  
573 doi:10.1029/2008GL035764, 2008.
- 574 Bey, I., Jacob, D. J., Logan, J. A., and Yantosca, R. M.: Asian chemical outflow to the  
575 Pacific in spring: Origins, pathways, and budgets, *J. Geophys. Res.-Atmos.*, 106, 23097-  
576 23113, 2001.
- 577 Bond, T. C., Bhardwaj, E., Dong, R., Jogani, R., Jung, S. K., Roden, C., Streets, D. G.,  
578 and Trautmann, N. M.: Historical emissions of black and organic carbon aerosol from  
579 energy-related combustion, 1850-2000, *Glob. Biogeochem. Cycle*, 21, Gb2018,  
580 doi:10.1029/2006GB002840, 2007.
- 581 Brock, C. A., Cozic, J., Bahreini, R., Froyd, K. D., Middlebrook, A. M., McComiskey, A.,  
582 Brioude, J., Cooper, O. R., Stohl, A., Aikin, K. C., de Gouw, J. A., Fahey, D. W., Ferrare,  
583 R. A., Gao, R. S., Gore, W., Holloway, J. S., Hubler, G., Jefferson, A., Lack, D. A.,  
584 Lance, S., Moore, R. H., Murphy, D. M., Nenes, A., Novelli, P. C., Nowak, J. B., Ogren,  
585 J. A., Peischl, J., Pierce, R. B., Pilewskie, P., Quinn, P. K., Ryerson, T. B., Schmidt, K. S.,  
586 Schwarz, J. P., Sodemann, H., Spackman, J. R., Stark, H., Thomson, D. S., Thornberry,  
587 T., Veres, P., Watts, L. A., Warneke, C., and Wollny, A. G.: Characteristics, sources, and  
588 transport of aerosols measured in spring 2008 during the aerosol, radiation, and cloud  
589 processes affecting Arctic Climate (ARCPAC) Project, *Atmos. Chem. Phys.*, 11, 2423-  
590 2453, doi:10.5194/acp-11-2423-2011, 2011.

591 Chen, Y. L., Kreidenweis, S. M., McInnes, L. M., Rogers, D. C., and DeMott, P. J.:  
592 Single particle analyses of ice nucleating aerosols in the upper troposphere and lower  
593 stratosphere, *Geophys. Res. Lett.*, 25, 1391-1394, 1998.

594 Chung, S. H., and Seinfeld, J. H.: Global distribution and climate forcing of carbonaceous  
595 aerosols, *J. Geophys. Res.-Atmos.*, 107, 4407, doi:10.1029/2001JD001397, 2002.

596 Cooke, W. F., Liousse, C., Cachier, H., and Feichter, J.: Construction of a 1 degrees x 1  
597 degrees fossil fuel emission data set for carbonaceous aerosol and implementation and  
598 radiative impact in the ECHAM4 model, *J. Geophys. Res.-Atmos.*, 104, 22137-22162,  
599 1999.

600 Cozic, J., Mertes, S., Verheggen, B., Cziczo, D. J., Gallavardin, S. J., Walter, S.,  
601 Baltensperger, U., and Weingartner, E.: Black carbon enrichment in atmospheric ice  
602 particle residuals observed in lower tropospheric mixed phase clouds, *J. Geophys. Res.-*  
603 *Atmos.*, 113, D15209, doi:10.1029/2007JD009266, 2008.

604 Croft, B., Lohmann, U., Martin, R. V., Stier, P., Wurzler, S., Feichter, J., Posselt, R., and  
605 Ferrachat, S.: Aerosol size-dependent below-cloud scavenging by rain and snow in the  
606 ECHAM5-HAM, *Atmos. Chem. Phys.*, 9, 4653-4675, 2009.

607 Dana, M. T., and Hales, J. M.: Statistical aspects of washout of polydisperse aerosols,  
608 *Atmos. Environ.*, 10, 45-50, 1976.

609 DelGenio, A. D., Yao, M. S., Kovari, W., and Lo, K. K. W.: A prognostic cloud water  
610 parameterization for global climate models, *J. Climate.*, 9, 270-304, 1996.

611 Djupstrom, M., Pacyna, J. M., Maenhaut, W., Winchester, J. W., Li, S. M., and Shaw, G.  
612 E.: Contamination of arctic air at 3 sites during a haze event in late winter 1986, *Atmos.*  
613 *Environ. Part A-General Topics*, 27, 2999-3010, 1993.

614 Doherty, S. J., Warren, S. G., Grenfell, T. C., Clarke, A. D., and Brandt, R. E.: Light-  
615 absorbing impurities in Arctic snow, *Atmos. Chem. Phys. Discuss.*, 10, 18807-18878,  
616 2010.

617 Dunlea, E. J., DeCarlo, P. F., Aiken, A. C., Kimmel, J. R., Peltier, R. E., Weber, R. J.,  
618 Tomlinson, J., Collins, D. R., Shinozuka, Y., McNaughton, C. S., Howell, S. G., Clarke,  
619 A. D., Emmons, L. K., Apel, E. C., Pfister, G. G., van Donkelaar, A., Martin, R. V.,  
620 Millet, D. B., Heald, C. L., and Jimenez, J. L.: Evolution of Asian aerosols during  
621 transpacific transport in INTEX-B, *Atmos. Chem. Phys.*, 9, 7257-7287, 2009.

622 Eleftheriadis, K., Vratolis, S., and Nyeki, S.: Aerosol black carbon in the European Arctic:  
623 Measurements at Zeppelin station, Ny-Alesund, Svalbard from 1998-2007, *Geophys. Res.*  
624 *Lett.*, 36, L02809, doi:10.1029/2008GL035741, 2009.

625 Feng, J.: A 3-mode parameterization of below-cloud scavenging of aerosols for use in  
626 atmospheric dispersion models, *Atmos. Environ.*, 41, 6808-6822,  
627 doi:10.1016/j.atmosenv.2007.04.046, 2007.

- 628 Feng, J.: A size-resolved model for below-cloud scavenging of aerosols by snowfall, *J.*  
629 *Geophys. Res.-Atmos.*, 114, D08203, doi:10.1029/2008JD011012, 2009.
- 630 Fisher, J. A., Jacob, D. J., Purdy, M. T., Kopacz, M., Le Sager, P., Carouge, C., Holmes,  
631 C. D., Yantosca, R. M., Batchelor, R. L., Strong, K., Diskin, G. S., Fuelberg, H. E.,  
632 Holloway, J. S., Hyer, E. J., McMillan, W. W., Warner, J., Streets, D. G., Zhang, Q.,  
633 Wang, Y., and Wu, S.: Source attribution and interannual variability of Arctic pollution  
634 in spring constrained by aircraft (ARCTAS, ARCPAC) and satellite (AIRS) observations  
635 of carbon monoxide, *Atmos. Chem. Phys.*, 10, 977-996, 2010.
- 636 Fisher, J. A., Jacob, D. J., Wang, Q., Bahreini, R., Carouge, C. C., Cubison, M. J., Dibb, J.  
637 E., Diehl, T., Jimenez, J. L., Leibensperger, E. M., Meinders, M. B. J., Pye, H. O. T.,  
638 Quinn, P. K., Sharma, S., van Donkelaar, A., and Yantosca, R. M.: Sources, distribution,  
639 and acidity of sulfate-ammonium aerosol in the Arctic in winter-spring, in review for  
640 *Atmos. Environ.*, 2011.
- 641 Flanner, M. G., Zender, C. S., Randerson, J. T., and Rasch, P. J.: Present-day climate  
642 forcing and response from black carbon in snow, *J. Geophys. Res.-Atmos.*, 112, D11202,  
643 doi:10.1029/2006JD008003, 2007.
- 644 Forster, P., Ramaswamy, V., Artaxo, P., Berntsen, T., Betts, R., Fahey, D. W., Haywood,  
645 J., Lean, J., Lowe, D. C., Myhre, G., Nganga, J., Prinn, R., Raga, G., Schulz, M., and Van  
646 Dorland, R.: Changes in Atmospheric Constituents and in Radiative Forcing. In: *Climate*  
647 *Change 2007: The Physical Science Basis. Contribution of Working Group I to the*  
648 *Fourth Assessment Report of the Intergovernmental Panel on Climate Change* [Solomon,  
649 S., D. Qin, M. Manning, Z. Chen, M. Marquis, K.B. Averyt, M. Tignor and H.L. Miller  
650 (eds.)]. Cambridge University Press, Cambridge, United Kingdom and New York, NY,  
651 USA., 2007.
- 652 Frossard, A. A., Shaw, P. M., Russell, L. M., Kroll, J. H., Canagaratna, M. R., Worsnop,  
653 D. R., Quinn, P. K., and Bates, T. S.: Springtime Arctic haze contributions of submicron  
654 organic particles from European and Asian combustion sources, *J. Geophys. Res.-Atmos.*,  
655 116, D05205, doi:10.1029/2010JD015178, 2011.
- 656 Fu, T. M., Jacob, D. J., Wittrock, F., Burrows, J. P., Vrekoussis, M., and Henze, D. K.:  
657 Global budgets of atmospheric glyoxal and methylglyoxal, and implications for  
658 formation of secondary organic aerosols, *J. Geophys. Res.-Atmos.*, 113, D15303,  
659 doi:10.1029/2007JD009505, 2008.
- 660 Fu, T. M., Jacob, D. J., and Heald, C. L.: Aqueous-phase reactive uptake of dicarbonyls  
661 as a source of organic aerosol over eastern North America, *Atmos. Environ.*, 43, 1814-  
662 1822, doi:10.1016/j.atmosenv.2008.12.029, 2009.
- 663 Giorgi, F., and Chameides, W. L.: Rainout lifetimes of highly soluble aerosols and gases  
664 as inferred from simulations with a general-circulation model, *J. Geophys. Res.-Atmos.*,  
665 91, 14367-14376, 1986.
- 666 Gong, S. L., Zhao, T. L., Sharma, S., Toom-Saunty, D., Lavoue, D., Zhang, X. B.,  
667 Leaitch, W. R., and Barrie, L. A.: Identification of trends and interannual variability of

668 sulfate and black carbon in the Canadian High Arctic: 1981-2007, *J. Geophys. Res.-*  
669 *Atmos.*, 115, D07305, doi:10.1029/2009JD012943, 2010.

670 Hegg, D. A., Warren, S. G., Grenfell, T. C., Doherty, S. J., Larson, T. V., and Clarke, A.  
671 D.: Source attribution of black carbon in arctic snow, *Environ. Sci. Technol.*, 43, 4016-  
672 4021, doi:10.1021/es803623f, 2009.

673 Hegg, D. A., Warren, S. G., Grenfell, T. C., Doherty, S. J., and Clarke, A. D.: Sources of  
674 light-absorbing aerosol in arctic snow and their seasonal variation, *Atmos. Chem. Phys.*,  
675 10, 10923-10938, doi:10.5194/acp-10-10923-2010, 2010.

676 Held, A., Orsini, D. A., Vaattovaara, P., Tjernström, M., and Leck, C.: Near-surface  
677 profiles of aerosol number concentration and temperature over the Arctic Ocean, *Atmos.*  
678 *Meas. Tech. Discuss.*, 4, 3017-3053, doi:10.5194/amtd-4-3017-2011, 2011.

679 Henze, D. K., and Seinfeld, J. H.: Global secondary organic aerosol from isoprene  
680 oxidation, *Geophys. Res. Lett.*, 33, L09812, doi:10.1029/2006GL025976, 2006.

681 Henze, D. K., Seinfeld, J. H., Ng, N. L., Kroll, J. H., Fu, T. M., Jacob, D. J., and Heald, C.  
682 L.: Global modeling of secondary organic aerosol formation from aromatic hydrocarbons:  
683 high- vs. low-yield pathways, *Atmos. Chem. Phys.*, 8, 2405-2420, 2008.

684 Hirdman, D., Burkhart, J. F., Sodemann, H., Eckhardt, S., Jefferson, A., Quinn, P. K.,  
685 Sharma, S., Strom, J., and Stohl, A.: Long-term trends of black carbon and sulphate  
686 aerosol in the Arctic: changes in atmospheric transport and source region emissions,  
687 *Atmos. Chem. Phys.*, 10, 9351-9368, doi:10.5194/acp-10-9351-2010, 2010.

688 Holmes, C. D., Jacob, D. J., Corbitt, E. S., Mao, J., Yang, X., Talbot, R., and Slemr, F.:  
689 Global atmospheric model for mercury including oxidation by bromine atoms, *Atmos.*  
690 *Chem. Phys.*, 10, 12037-12057, doi:10.5194/acp-10-12037-2010, 2010.

691 Huang, L., Gong, S. L., Jia, C. Q., and Lavoue, D.: Importance of deposition processes in  
692 simulating the seasonality of the Arctic black carbon aerosol, *J. Geophys. Res.-Atmos.*,  
693 115, D17207, doi:10.1029/2009JD013478, 2010a.

694 Huang, L., Gong, S. L., Jia, C. Q., and Lavoue, D.: Relative contributions of  
695 anthropogenic emissions to black carbon aerosol in the Arctic, *J. Geophys. Res.-Atmos.*,  
696 115, D19208, doi:10.1029/2009JD013592, 2010b.

697 IEA: Energy Statistics of Non-OECD Countries 2010, OECD Publishing, 2010.

698 Jacob, D. J., Crawford, J. H., Maring, H., Clarke, A. D., Dibb, J. E., Emmons, L. K.,  
699 Ferrare, R. A., Hostetler, C. A., Russell, P. B., Singh, H. B., Thompson, A. M., Shaw, G.  
700 E., McCauley, E., Pederson, J. R., and Fisher, J. A.: The arctic research of the  
701 composition of the troposphere from aircraft and satellites (ARCTAS) mission: design,  
702 execution, and first results, *Atmos. Chem. Phys.*, 10, 5191-5212, doi:10.5194/acp-10-  
703 5191-2010, 2010.

704 Jacobson, M. Z.: Strong radiative heating due to the mixing state of black carbon in  
705 atmospheric aerosols, *Nature*, 409, 695-697, 2001.

706 Jimenez, J., Jayne, J., Shi, Q., Kolb, C., Worsnop, D., Yourshaw, I., Seinfeld, J., Flagan,  
707 R., Zhang, X., and Smith, K.: Ambient aerosol sampling using the Aerodyne Aerosol  
708 Mass Spectrometer, *J. Geophys. Res.*, 108, 8425, 2003.

709 Karcher, B., Mohler, O., DeMott, P. J., Pechtl, S., and Yu, F.: Insights into the role of  
710 soot aerosols in cirrus cloud formation, *Atmos. Chem. Phys.*, 7, 4203-4227, 2007.

711 Kawamura, K., Kasukabe, H., and Barrie, L. A.: Source and reaction pathways of  
712 dicarboxylic acids, ketoacids and dicarbonyls in arctic aerosols: One year of observations,  
713 *Atmos. Environ.*, 30, 1709-1722, 1996.

714 Klonecki, A., Hess, P., Emmons, L., Smith, L., Orlando, J., and Blake, D.: Seasonal  
715 changes in the transport of pollutants into the Arctic troposphere-model study, *J. Geophys.*  
716 *Res.-Atmos.*, 108, 8367, doi:10.1029/2002JD002199, 2003.

717 Koch, D., and Hansen, J.: Distant origins of Arctic black carbon: A Goddard Institute for  
718 Space Studies ModelE experiment, *J. Geophys. Res.-Atmos.*, 110, D04204,  
719 doi:10.1029/2004JD005296, 2005.

720 Koch, D., Bond, T. C., Streets, D., Unger, N., and van der Werf, G. R.: Global impacts of  
721 aerosols from particular source regions and sectors, *J. Geophys. Res.-Atmos.*, 112,  
722 D02205, doi:10.1029/2005JD007024, 2007.

723 Koch, D., Menon, S., Del Genio, A., Ruedy, R., Alienov, I., and Schmidt, G. A.:  
724 Distinguishing aerosol impacts on climate over the past century, *J. Climate*, 22, 2659-  
725 2677, doi:10.1175/2008JCLI2573.1, 2009a.

726 Koch, D., Schulz, M., Kinne, S., McNaughton, C., Spackman, J. R., Balkanski, Y., Bauer,  
727 S., Bernsten, T., Bond, T. C., Boucher, O., Chin, M., Clarke, A., De Luca, N., Dentener,  
728 F., Diehl, T., Dubovik, O., Easter, R., Fahey, D. W., Feichter, J., Fillmore, D., Freitag, S.,  
729 Ghan, S., Ginoux, P., Gong, S., Horowitz, L., Iversen, T., Kirkevåg, A., Klimont, Z.,  
730 Kondo, Y., Krol, M., Liu, X., Miller, R., Montanaro, V., Moteki, N., Myhre, G., Penner, J.  
731 E., Perlwitz, J., Pitari, G., Reddy, S., Sahu, L., Sakamoto, H., Schuster, G., Schwarz, J. P.,  
732 Seland, O., Stier, P., Takegawa, N., Takemura, T., Textor, C., van Aardenne, J. A., and  
733 Zhao, Y.: Evaluation of black carbon estimations in global aerosol models, *Atmos. Chem.*  
734 *Phys.*, 9, 9001-9026, 2009b.

735 Kondo, Y., Matsui, H., Moteki, N., Sahu, L., Takegawa, N., Kajino, M., Zhao, Y.,  
736 Cubison, M. J., Jimenez, J. L., Vay, S., Diskin, G. S., Anderson, B., Wisthaler, A.,  
737 Mikoviny, T., Fuelberg, H. E., Blake, D. R., Huey, G., Weinheimer, A. J., Knapp, D. J.,  
738 and Brune, W. H.: Emissions of black carbon, organic, and inorganic aerosols from  
739 biomass burning in North America and Asia in 2008, *J. Geophys. Res.-Atmos.*, 116,  
740 D08204, doi:10.1029/2010JD015152, 2011.

741 Kristjansson, J. E., Iversen, T., Kirkevåg, A., Seland, O., and Debernard, J.: Response of  
742 the climate system to aerosol direct and indirect forcing: Role of cloud feedbacks, *J.*  
743 *Geophys. Res.-Atmos.*, 110, D24206, doi:10.1029/2005JD006299, 2005.

744 Law, K. S., and Stohl, A.: Arctic air pollution: Origins and impacts, *Science*, 315, 1537-  
745 1540, doi:10.1126/science.1137695, 2007.

746 Leibensperger, E. M., Mickley, L. J., Jacob, D. J., Chen, W.-T., Seinfeld, J. H., Nenes, A.,  
747 Adams, P. J., Streets, D. G., Kumar, N., and Rind, D.: Climatic effects of 1950-2050  
748 changes in US anthropogenic aerosols - Part 1: Aerosol trends and radiative forcing,  
749 submitted to *Atmos. Chem. Phys.*, 2011.

750 Liu, H. Y., Jacob, D. J., Bey, I., and Yantosca, R. M.: Constraints from Pb-210 and Be-7  
751 on wet deposition and transport in a global three-dimensional chemical tracer model  
752 driven by assimilated meteorological fields, *J. Geophys. Res.-Atmos.*, 106, 12109-12128,  
753 2001.

754 Liu, H. Y., Jacob, D. J., Bey, I., Yantosca, R. M., Duncan, B. N., and Sachse, G. W.:  
755 Transport pathways for Asian pollution outflow over the Pacific: Interannual and  
756 seasonal variations, *J. Geophys. Res.-Atmos.*, 108, 8786, doi:10.1029/2002JD003102,  
757 2003.

758 Lu, Z., Streets, D. G., Zhang, Q., Wang, S., Carmichael, G. R., Cheng, Y. F., Wei, C.,  
759 Chin, M., Diehl, T., and Tan, Q.: Sulfur dioxide emissions in China and sulfur trends in  
760 East Asia since 2000, *Atmos. Chem. Phys.*, 10, 6311-6331, doi:10.5194/acp-10-6311-  
761 2010, 2010.

762 Mao, J., Jacob, D. J., Evans, M. J., Olson, J. R., Ren, X., Brune, W. H., St. Clair, J. M.,  
763 Crouse, J. D., Spencer, K. M., Beaver, M. R., Wennberg, P. O., Cubison, M. J., Jimenez,  
764 J. L., Fried, A., Weibring, P., Walega, J. G., Hall, S. R., Weinheimer, A. J., Cohen, R. C.,  
765 Chen, G., Crawford, J. H., McNaughton, C., Clarke, A. D., Jaeglé L., Fisher, J. A.,  
766 Yantosca, R. M., Le Sager, P., and Carouge, C.: Chemistry of hydrogen oxide radicals  
767 (HOx) in the Arctic troposphere in spring, *Atmos. Chem. Phys.*, 10, 5823-5838,  
768 doi:10.5194/acp-10-5823-2010, 2010.

769 Matsui, H., Kondo, Y., Moteki, N., Takegawa, N., Sahu, L. K., Zhao, Y., Fuelberg, H. E.,  
770 Sessions, W. R., Diskin, G., Blake, D. R., Wisthaler, A., and Koike, M.: Seasonal  
771 variation of the transport of black carbon aerosol from the Asian continent to the Arctic  
772 during the ARCTAS aircraft campaign, *J. Geophys. Res.-Atmos.*, 116, D05202,  
773 doi:10.1029/2010JD015067, 2011.

774 Mc Naughton, C. S., Clarke, A. D., Freitag, S., Kapustin, V. N., Kondo, Y., Moteki, N.,  
775 Sahu, L., Takegawa, N., Schwarz, J. P., Spackman, J. R., Watts, L., Diskin, G., Podolske,  
776 J., Holloway, J. S., Wisthaler, A., Mikoviny, T., de Gouw, J., Warneke, C., Jimenez, J.,  
777 Cubison, M., Howell, S. G., Middlebrook, A., Bahreini, R., Anderson, B. E., Winstead,  
778 E., Thornhill, K. L., Lack, D., Cozic, J., and Brock, C. A.: Absorbing aerosol in the  
779 troposphere of the Western Arctic during the 2008 ARCTAS/ARCPAC airborne field  
780 campaigns, *Atmos. Chem. Phys. Discuss.*, 11, 1543-1594, doi:10.5194/acpd-11-1543-  
781 2011, 2011.

782 McConnell, J. R., Edwards, R., Kok, G. L., Flanner, M. G., Zender, C. S., Saltzman, E. S.,  
783 Banta, J. R., Pasteris, D. R., Carter, M. M., and Kahl, J. D. W.: 20th-century industrial

784 black carbon emissions altered arctic climate forcing, *Science*, 317, 1381-1384,  
785 doi:10.1126/science.1144856, 2007.

786 Murakami, M., Kimura, T., Magono, C., and Kikuchi, K.: Observations of precipitation  
787 scavenging for water-soluble particles, *J. Meteorol. Soc. Jap.*, 61, 346-358, 1983.

788 Nilsson, E. D., and Rannik, U.: Turbulent aerosol fluxes over the Arctic Ocean 1. Dry  
789 deposition over sea and pack ice, *J. Geophys. Res.-Atmos.*, 106, 32125-32137, 2001.

790 Park, R. J., Jacob, D. J., Chin, M., and Martin, R. V.: Sources of carbonaceous aerosols  
791 over the United States and implications for natural visibility, *J. Geophys. Res.-Atmos.*,  
792 108, 4355, doi:10.1029/2002JD003190, 2003.

793 Park, R. J., Jacob, D. J., Palmer, P. I., Clarke, A. D., Weber, R. J., Zondlo, M. A., Eisele,  
794 F. L., Bandy, A. R., Thornton, D. C., Sachse, G. W., and Bond, T. C.: Export efficiency  
795 of black carbon aerosol in continental outflow: Global implications, *J. Geophys. Res.-*  
796 *Atmos.*, 110, D11205, doi:10.1029/2004JD005432, 2005.

797 Park, R. J., Jacob, D. J., Kumar, N., and Yantosca, R. M.: Regional visibility statistics in  
798 the United States: Natural and transboundary pollution influences, and implications for  
799 the Regional Haze Rule, *Atmos. Environ.*, 40, 5405-5423,  
800 doi:10.1016/j.atmosenv.2006.04.059, 2006.

801 Quinn, P. K., Miller, T. L., Bates, T. S., Ogren, J. A., Andrews, E., and Shaw, G. E.: A 3-  
802 year record of simultaneously measured aerosol chemical and optical properties at  
803 Barrow, Alaska, *J. Geophys. Res.-Atmos.*, 107, 4130, doi:10.1029/2001JD001248, 2002.

804 Quinn, P. K., Shaw, G., Andrews, E., Dutton, E. G., Ruoho-Airola, T., and Gong, S. L.:  
805 Arctic haze: current trends and knowledge gaps, *Tellus. B*, 59, 99-114,  
806 doi:10.1111/j.1600-0889.2006.00238.x, 2007.

807 Quinn, P. K., Bates, T. S., Baum, E., Doubleday, N., Fiore, A. M., Flanner, M., Fridlind,  
808 A., Garrett, T. J., Koch, D., Menon, S., Shindell, D., Stohl, A., and Warren, S. G.: Short-  
809 lived pollutants in the Arctic: their climate impact and possible mitigation strategies,  
810 *Atmos. Chem. Phys.*, 8, 1723-1735, 2008.

811 Rastigejev, Y., Park, R., Brenner, M. P., and Jacob, D. J.: Resolving intercontinental  
812 pollution plumes in global models of atmospheric transport, *J. Geophys. Res.*, 115,  
813 D02302, doi:10.1029/2009JD012568, 2010.

814 Reddy, M. S., and Boucher, O.: A study of the global cycle of carbonaceous aerosols in  
815 the LMDZT general circulation model, *J. Geophys. Res.-Atmos.*, 109, D14202,  
816 doi:10.1029/2003JD004048, 2004.

817 Reid, J. S., Koppmann, R., Eck, T. F., and Eleuterio, D. P.: A review of biomass burning  
818 emissions part II: intensive physical properties of biomass burning particles, *Atmos.*  
819 *Chem. Phys.*, 5, 799-825, 2005.

820 Reid, J. S., Hyer, E. J., Prins, E. M., Westphal, D. L., Zhang, J. L., Wang, J., Christopher,  
821 S. A., Curtis, C. A., Schmidt, C. C., Eleuterio, D. P., Richardson, K. A., and Hoffman, J.

822 P.: Global monitoring and forecasting of biomass-burning smoke: description of and  
823 lessons from the fire locating and modeling of burning emissions (FLAMBE) program,  
824 IEEE J. Sel. Top. Appl., 2(3), 144-162, doi:10.1109/JSTARS.2009.2027443, 2009.

825 Ricard, V., Jaffrezo, J. L., Kerminen, V. M., Hillamo, R. E., Sillanpaa, M., Ruellan, S.,  
826 Lioussé, C., and Cachier, H.: Two years of continuous aerosol measurements in northern  
827 Finland, *J. Geophys. Res.-Atmos.*, 107, 4129, doi:10.1029/2001JD000952, 2002.

828 Sharma, S., Andrews, E., Barrie, L. A., Ogren, J. A., and Lavoue, D.: Variations and  
829 sources of the equivalent black carbon in the high Arctic revealed by long-term  
830 observations at Alert and Barrow: 1989-2003, *J. Geophys. Res.-Atmos.*, 111, D14208,  
831 doi:10.1029/2005JD006581, 2006.

832 Shaw, G. E.: Evidence for a central Eurasian source area of Arctic haze in Alaska, *Nature*,  
833 299, 815-818, 1982.

834 Shaw, P. M., Russell, L. M., Jefferson, A., and Quinn, P. K.: Arctic organic aerosol  
835 measurements show particles from mixed combustion in spring haze and from frost  
836 flowers in winter, *Geophys. Res. Lett.*, 37, L10803, doi:10.1029/2010GL042831, 2010.

837 Shindell, D. T., Chin, M., Dentener, F., Doherty, R. M., Faluvegi, G., Fiore, A. M., Hess,  
838 P., Koch, D. M., MacKenzie, I. A., Sanderson, M. G., Schultz, M. G., Schulz, M.,  
839 Stevenson, D. S., Teich, H., Textor, C., Wild, O., Bergmann, D. J., Bey, I., Bian, H.,  
840 Cuvelier, C., Duncan, B. N., Folberth, G., Horowitz, L. W., Jonson, J., Kaminski, J. W.,  
841 Marmer, E., Park, R., Pringle, K. J., Schroeder, S., Szopa, S., Takemura, T., Zeng, G.,  
842 Keating, T. J., and Zuber, A.: A multi-model assessment of pollution transport to the  
843 Arctic, *Atmos. Chem. Phys.*, 8, 5353-5372, 2008.

844 Spackman, J. R., Gao, R. S., Neff, W. D., Schwarz, J. P., Watts, L. A., Fahey, D. W.,  
845 Holloway, J. S., Ryerson, T. B., Peischl, J., and Brock, C. A.: Aircraft observations of  
846 enhancement and depletion of black carbon mass in the springtime Arctic, *Atmos. Chem.*  
847 *Phys.*, 10, 9667-9680, doi:10.5194/acp-10-9667-2010, 2010.

848 Stohl, A.: Characteristics of atmospheric transport into the Arctic troposphere, *J.*  
849 *Geophys. Res.-Atmos.*, 111, D11306, doi:10.1029/2005JD006888, 2006.

850 Stohl, A., Berg, T., Burkhardt, J. F., Fjaeraa, A. M., Forster, C., Herber, A., Hov, O.,  
851 Lunder, C., McMillan, W. W., Oltmans, S., Shiobara, M., Simpson, D., Solberg, S.,  
852 Stebel, K., Strom, J., Torseth, K., Treffeisen, R., Virkkunen, K., and Yttri, K. E.: Arctic  
853 smoke - record high air pollution levels in the European Arctic due to agricultural fires in  
854 Eastern Europe in spring 2006, *Atmos. Chem. Phys.*, 7, 511-534, 2007.

855 Targino, A. C., Coe, H., Cozic, J., Crosier, J., Crawford, I., Bower, K., Flynn, M.,  
856 Gallagher, M., Allan, J., Verheggen, B., Weingartner, E., Baltensperger, U., and  
857 Choulaton, T.: Influence of particle chemical composition on the phase of cold clouds at  
858 a high-alpine site in Switzerland, *J. Geophys. Res.-Atmos.*, 114, D18206,  
859 doi:10.1029/2008JD011365, 2009.

860 Tilmes, S., Emmons, L. K., Law, K. S., Ancellet, G., Schlager, H., Paris, J. D., Fuelberg,  
861 H. E., Streets, D. G., Wiedinmyer, C., Diskin, G. S., Kondo, Y., Holloway, J., Schwarz, J.  
862 P., Spackman, J. R., Campos, T., Néédéc, P., and Panchenko, M. V.: Source  
863 contributions to Northern Hemisphere CO and black carbon during spring and summer  
864 2008 from POLARCAT and START08/preHIPPO observations and MOZART-4, *Atmos.*  
865 *Chem. Phys. Discuss.*, 11, 5935-5983, doi:10.5194/acpd-11-5935-2011, 2011.

866 Turpin, B. J., and Lim, H. J.: Species contributions to PM<sub>2.5</sub> mass concentrations:  
867 Revisiting common assumptions for estimating organic mass, *Aerosol Sci. Tech.*, 35,  
868 602-610, 2001.

869 van der Werf, G. R., Randerson, J. T., Giglio, L., Collatz, G. J., Kasibhatla, P. S., and  
870 Arellano, A. F.: Interannual variability in global biomass burning emissions from 1997 to  
871 2004, *Atmos. Chem. Phys.*, 6, 3423-3441, 2006.

872 van Donkelaar, A., Martin, R. V., Leaitch, W. R., Macdonald, A. M., Walker, T. W.,  
873 Streets, D. G., Zhang, Q., Dunlea, E. J., Jimenez, J. L., Dibb, J. E., Huey, L. G., Weber,  
874 R., and Andreae, M. O.: Analysis of aircraft and satellite measurements from the  
875 Intercontinental Chemical Transport Experiment (INTEX-B) to quantify long-range  
876 transport of East Asian sulfur to Canada, *Atmos. Chem. Phys.*, 8, 2999-3014, 2008.

877 Wang, Y. H., Jacob, D. J., and Logan, J. A.: Global simulation of tropospheric O<sub>3</sub>-NO<sub>x</sub>-  
878 hydrocarbon chemistry 1. Model formulation, *J. Geophys. Res.-Atmos.*, 103, 10713-  
879 10725, 1998.

880 Warneke, C., Bahreini, R., Brioude, J., Brock, C. A., de Gouw, J. A., Fahey, D. W.,  
881 Froyd, K. D., Holloway, J. S., Middlebrook, A., Miller, L., Montzka, S., Murphy, D. M.,  
882 Peischl, J., Ryerson, T. B., Schwarz, J. P., Spackman, J. R., and Veres, P.: Biomass  
883 burning in Siberia and Kazakhstan as an important source for haze over the Alaskan  
884 Arctic in April 2008, *Geophys. Res. Lett.*, 36, L02813, doi:10.1029/2008GL036194,  
885 2009.

886 Warneke, C., Froyd, K. D., Brioude, J., Bahreini, R., Brock, C. A., Cozic, J., de Gouw, J.  
887 A., Fahey, D. W., Ferrare, R., Holloway, J. S., Middlebrook, A. M., Miller, L., Montzka,  
888 S., Schwarz, J. P., Sodemann, H., Spackman, J. R., and Stohl, A.: An important  
889 contribution to springtime Arctic aerosol from biomass burning in Russia, *Geophys. Res.*  
890 *Lett.*, 37, L01801, doi:10.1029/2009GL041816, 2010.

891 Warren, S. G., and Wiscombe, W. J.: Dirty snow after nuclear-war, *Nature*, 313, 467-470,  
892 1985.

893 Wesely, M. L.: Parameterization of surface resistances to gaseous dry deposition in  
894 regional-scale numerical-models, *Atmos. Environ.*, 23, 1293-1304, 1989.

895 Zhang, Q., Jimenez, J. L., Canagaratna, M. R., Allan, J. D., Coe, H., Ulbrich, I., Alfarra,  
896 M. R., Takami, A., Middlebrook, A. M., Sun, Y. L., Dzepina, K., Dunlea, E., Docherty,  
897 K., DeCarlo, P. F., Salcedo, D., Onasch, T., Jayne, J. T., Miyoshi, T., Shimono, A.,  
898 Hatakeyama, S., Takegawa, N., Kondo, Y., Schneider, J., Drewnick, F., Borrmann, S.,  
899 Weimer, S., Demerjian, K., Williams, P., Bower, K., Bahreini, R., Cottrell, L., Griffin, R.

900 J., Rautiainen, J., Sun, J. Y., Zhang, Y. M., and Worsnop, D. R.: Ubiquity and dominance  
901 of oxygenated species in organic aerosols in anthropogenically-influenced Northern  
902 Hemisphere midlatitudes, *Geophys. Res. Lett.*, 34, L13801, doi:10.1029/2007GL029979,  
903 2007.

904 Zhang, L., Jacob, D. J., Boersma, K. F., Jaffe, D. A., Olson, J. R., Bowman, K. W.,  
905 Worden, J. R., Thompson, A. M., Avery, M. A., Cohen, R. C., Dibb, J. E., Flock, F. M.,  
906 Fuelberg, H. E., Huey, L. G., McMillan, W. W., Singh, H. B., and Weinheimer, A. J.:  
907 Transpacific transport of ozone pollution and the effect of recent Asian emission  
908 increases on air quality in North America: an integrated analysis using satellite, aircraft,  
909 ozonesonde, and surface observations, *Atmos. Chem. Phys.*, 8, 6117-6136, 2008a.

910 Zhang, X. Y., Wang, Y. Q., Zhang, X. C., Guo, W., and Gong, S. L.: Carbonaceous  
911 aerosol composition over various regions of China during 2006, *J. Geophys. Res.-Atmos.*,  
912 113, D14111, doi:10.1029/2007JD009525, 2008b.

913 **Tables and figure captions**914 **Table 1.** Global GEOS-Chem emissions of carbonaceous aerosols in 2008<sup>a</sup>

Source	Black Carbon (Tg C a <sup>-1</sup> )	Organic Aerosol (Tg C a <sup>-1</sup> )
Anthropogenic <sup>b</sup>	7.0	14
North America (172.5–17.5 °W, 24–88 °N)	0.41	0.56
Europe (17.5 °W–30 °E, 50–88 °N & 17.5 °W–60 °E, 33–50 °N)	0.63	1.1
Russia (30–172.5 °E, 50–88 °N)	0.23	0.52
Asia (60–152.5 °E, 0–50 °N)	4.7	9.8
Rest of world	1.0	2.6
Open Fires <sup>c</sup>	11	84
North America (172.5–17.5 °W, 24–88 °N)	0.20	2.7
Europe (17.5 °W–30 °E, 33–88 °N)	0.082	0.63
Russia (30–152.5 °E, 33–60 °N)	0.60	4.5
South Asia (60–152.5 °E, 0–33 °N)	0.77	6.1
Rest of world	9.5	70
Total	18	98

<sup>a</sup> Values are annual means. Different region definitions are used for anthropogenic and open fire sources.

<sup>b</sup> Including fossil fuel and biofuel combustion. Values are from Bond et al. [2007] but with doubling of Russian and Asian emissions (see text).

<sup>c</sup> From the FLAMBE inventory of Reid et al. [2009] but with major modifications for Russian and Southeast Asian sources as described in the text.

915

916 **Figure 1.** GEOS-Chem emissions of black carbon (BC) and primary organic aerosol  
917 (POA) in April 2008. Annual regional totals are in Table 1.

918 **Figure 2.** Scatterplot of BC vs. OA concentrations in fire plumes diagnosed by  $[\text{CH}_3\text{CN}] >$   
919 200 ppt for the ensemble of ARCTAS DC-8 flights (1–19 April 2008). STP refers to  
920 standard conditions of temperature and pressure (273 K, 1 atm) so that  $\mu\text{g C m}^{-3}$  STP is a  
921 mixing ratio unit. The reduced-major-axis (RMA) regression is shown by the solid line  
922 and the corresponding equation is given inset.

923 **Figure 3.** Annual mean surface air concentrations of BC aerosol in China, Europe, and  
924 the US. Model results for 2008 (solid contours) are compared to observations (circles).  
925 Observations are from Zhang et al. [2008] in China for 2006, from the EMEP network in  
926 Europe for 2002–2003 (<http://tarantula.nilu.no/projects/ccc/emepdata.html>), and from the  
927 IMPROVE network in the US for 2008 ([http://vista.cira.colostate.edu/improve/Data-  
928 /IMPROVE/AsciiData.aspx](http://vista.cira.colostate.edu/improve/Data-IMPROVE/AsciiData.aspx)). Normalized mean bias (NMB) statistics for each region are  
929 shown inset.

930 **Figure 4.** DC-8 flight tracks during the April 2008 ARCTAS campaign (red lines). Long-  
931 term monitoring sites for BC at Barrow and Denali are also indicated.

932 **Figure 5.** Fine aerosol composition observed along the ARCTAS DC-8 flight tracks (1-  
933 19 April 2008), averaged over 2-km altitude bins. The averaging excludes data collected  
934 south of 60°N, in stratospheric air, and in biomass burning plumes (see text).

935 **Figure 6.** Scatterplots of simulated vs. observed BC and OA concentrations along the  
936 DC-8 flight tracks during ARCTAS (1-19 April 2008). Colors indicate the corresponding  
937 concentrations of CH<sub>3</sub>CN, a tracer of biomass burning. The 1:1 line is also shown.

938 **Figure 7.** Mean vertical profiles of BC and OA concentrations along the DC-8 flight  
939 tracks in ARCTAS (1-19 April 2008), averaged over 1-km altitude bins. The top panels  
940 compare observations to GEOS-Chem and separate the model contributions from  
941 anthropogenic and open fire sources. The bottom panel further separates model BC  
942 contributions by source regions. Anthropogenic sources include fossil fuel and biofuel  
943 combustion.

944 **Figure 8.** Scatterplots of BC and OA vs. sulfate (SO<sub>4</sub><sup>2-</sup>) concentrations in ARCTAS.  
945 Observations from the DC-8 aircraft (left panels) are compared to model values sampled  
946 along the aircraft flight tracks (right panels). Individual points are colored by altitude.  
947 Reduced-major-axis (RMA) regression statistics and linear fits are shown in thin black  
948 for near-surface data (<1 km) and in thick black for mid-tropospheric data (2-6 km).

949 **Figure 9.** Same as Fig. 8 but for BC vs. OA concentrations in ARCTAS.

950 **Figure 10.** Seasonal variation of BC and OA surface air concentrations at Denali and  
951 Barrow in Alaska. The thick black lines are monthly mean observations for 2008. The  
952 thin black lines are monthly mean observations for 2002-2008 with vertical bars  
953 representing interannual standard deviations. The thick line for OA at Barrow represents  
954 seasonal mean concentrations in Nov 2008-Feb 2009 and Mar-Jun 2008 from P. Shaw et  
955 al. (2010). Additive model contributions from different sources in the 2008 simulation are  
956 shown in color.

957 **Figure 11.** Contributions of open fire and anthropogenic (fuel combustion) sources to the  
958 BC deposition flux in GEOS-Chem for winter and spring 2008.

959 **Figure 12.** Simulated BC content of Arctic snow in winter and spring 2007-2009. Snow-  
960 free areas are shown in gray. Purple circles indicate snow sampling sites from Doherty et  
961 al. (2010) for the corresponding years and seasons.

962 **Figure 13.** Scatterplots of simulated vs. observed BC content in snow for North  
963 American and Russian Arctic sites in Mar-May 2007-2009 (Figure 12). Observations  
964 from Doherty et al. (2010) are averaged over model grid squares, and model results are  
965 sampled for the month and year of observations. The data are colored by latitude. Also  
966 shown is the 1:1 line.

967 **Figure 14.** Model decreases in snow albedo due to BC deposition in the Arctic (>60°N)  
968 in winter and spring 2008. Snow-free areas are shown in gray.

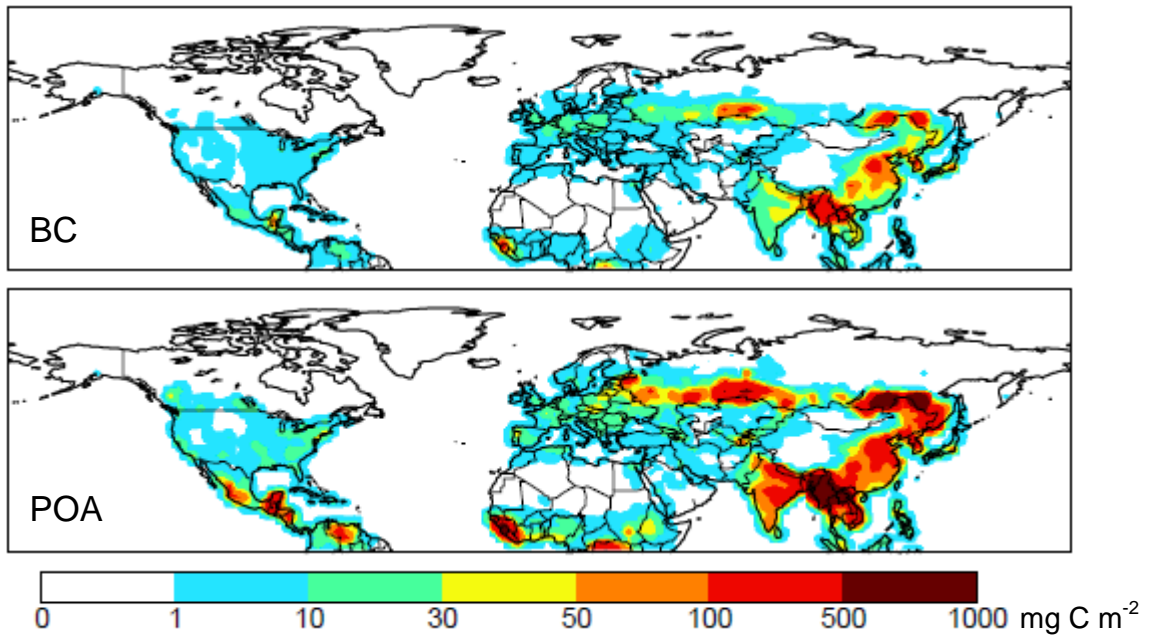


Fig. 1. GEOS-Chem emissions of black carbon (BC) and primary organic aerosol (POA) in April 2008. Annual regional totals are in Table 1.

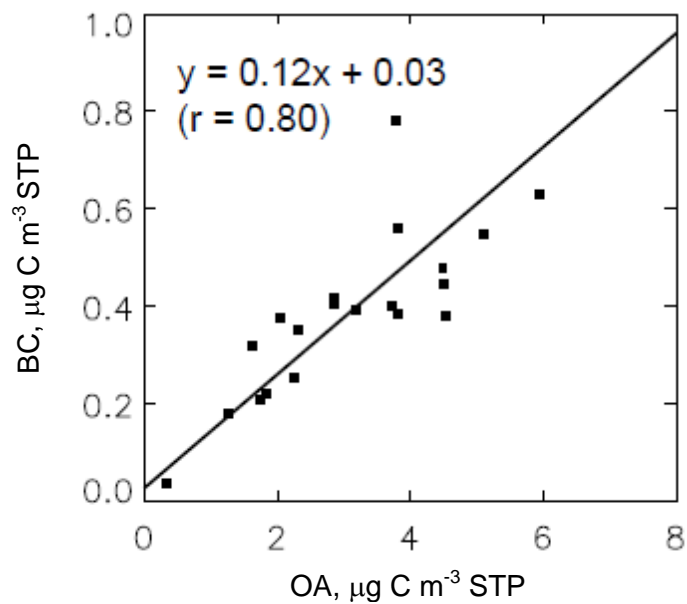


Fig. 2. Scatterplot of BC vs. OA concentrations in fire plumes diagnosed by  $[\text{CH}_3\text{CN}] > 200$  ppt for the ensemble of ARCTAS DC-8 flights (1-19 April 2008). STP refers to standard conditions of temperature and pressure (273 K, 1 atm) so that  $\mu\text{g C m}^{-3}$  STP is a mixing ratio unit. The reduced-major-axis (RMA) regression is shown by the solid line and the corresponding equation is given inset.

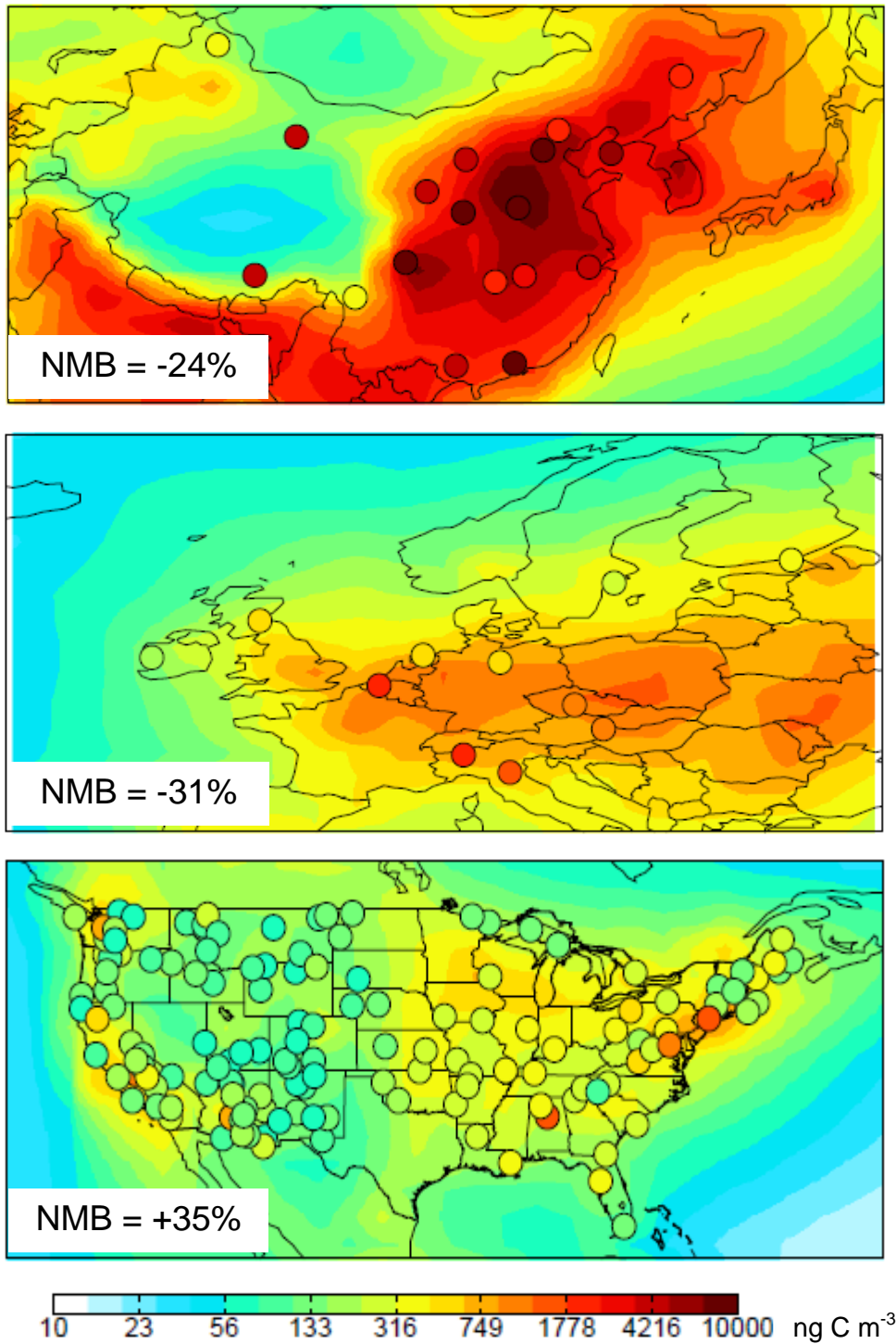


Fig.3. Annual mean surface air concentrations of BC aerosol in China, Europe, and the US. Model results for 2008 (solid contours) are compared to observations (circles). Observations are from Zhang et al. [2008] in China for 2006, from the EMEP network in Europe for 2002-2003 (<http://tarantula.nilu.no/projects/ccc/emepdata.html>), and from the IMPROVE network in the US for 2008 (<http://vista.cira.colostate.edu/improve/Data->

[/IMPROVE/AsciiData.aspx](#)). Normalized mean bias (NMB) statistics for each region are shown inset.



Fig. 4. DC-8 flight tracks during the April 2008 ARCTAS campaign (red lines). Long-term monitoring sites for BC at Barrow and Denali are also indicated.

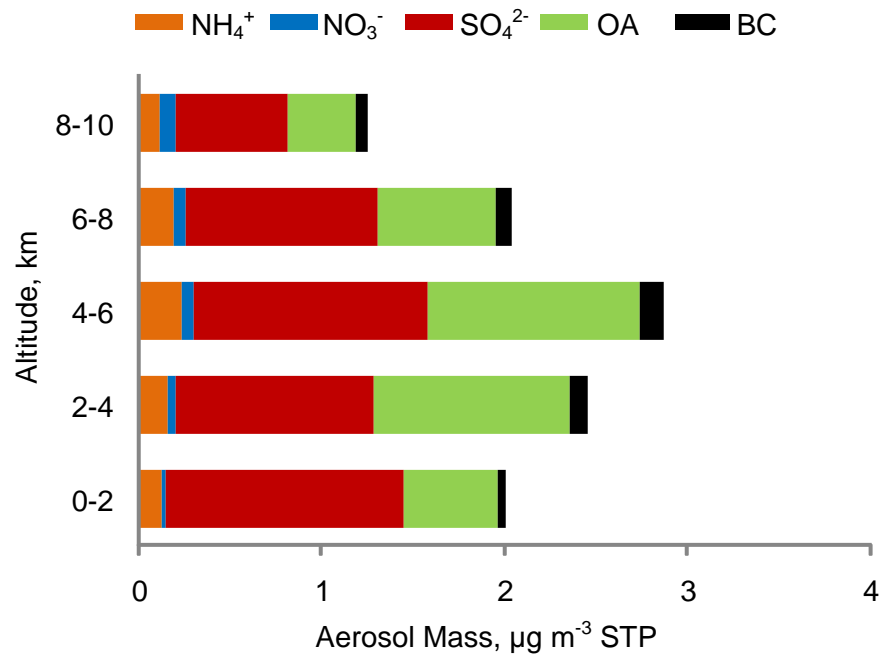


Fig. 5. Fine aerosol composition observed along the ARCTAS DC-8 flight tracks (1-19 April 2008), averaged over 2-km altitude bins. The averaging excludes data collected south of 60°N, in stratospheric air, and in biomass burning plumes (see text).

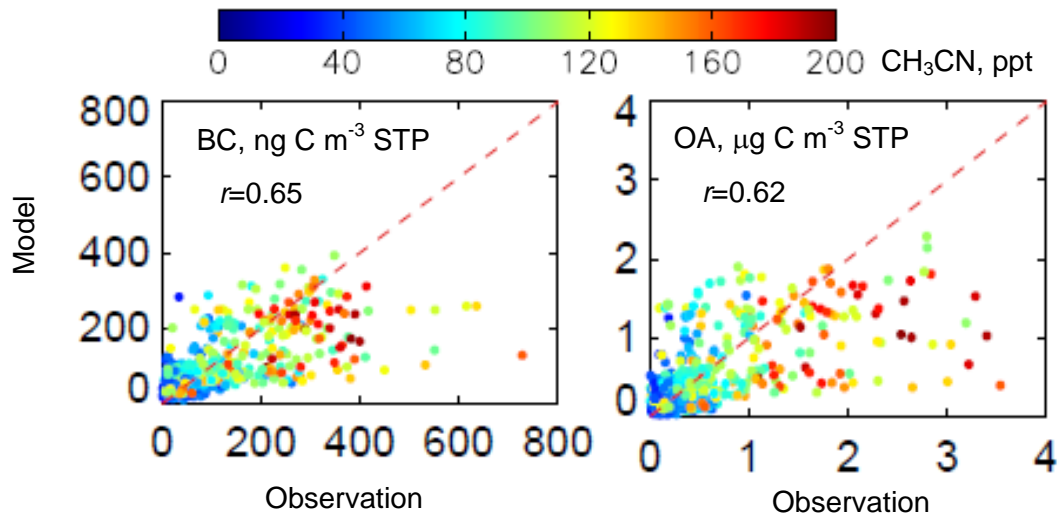


Fig. 6. Scatterplots of simulated vs. observed BC and OA concentrations along the DC-8 flight tracks during ARCTAS (1-19 April 2008). Colors indicate the corresponding concentrations of CH<sub>3</sub>CN, a tracer of biomass burning. The 1:1 line is also shown.

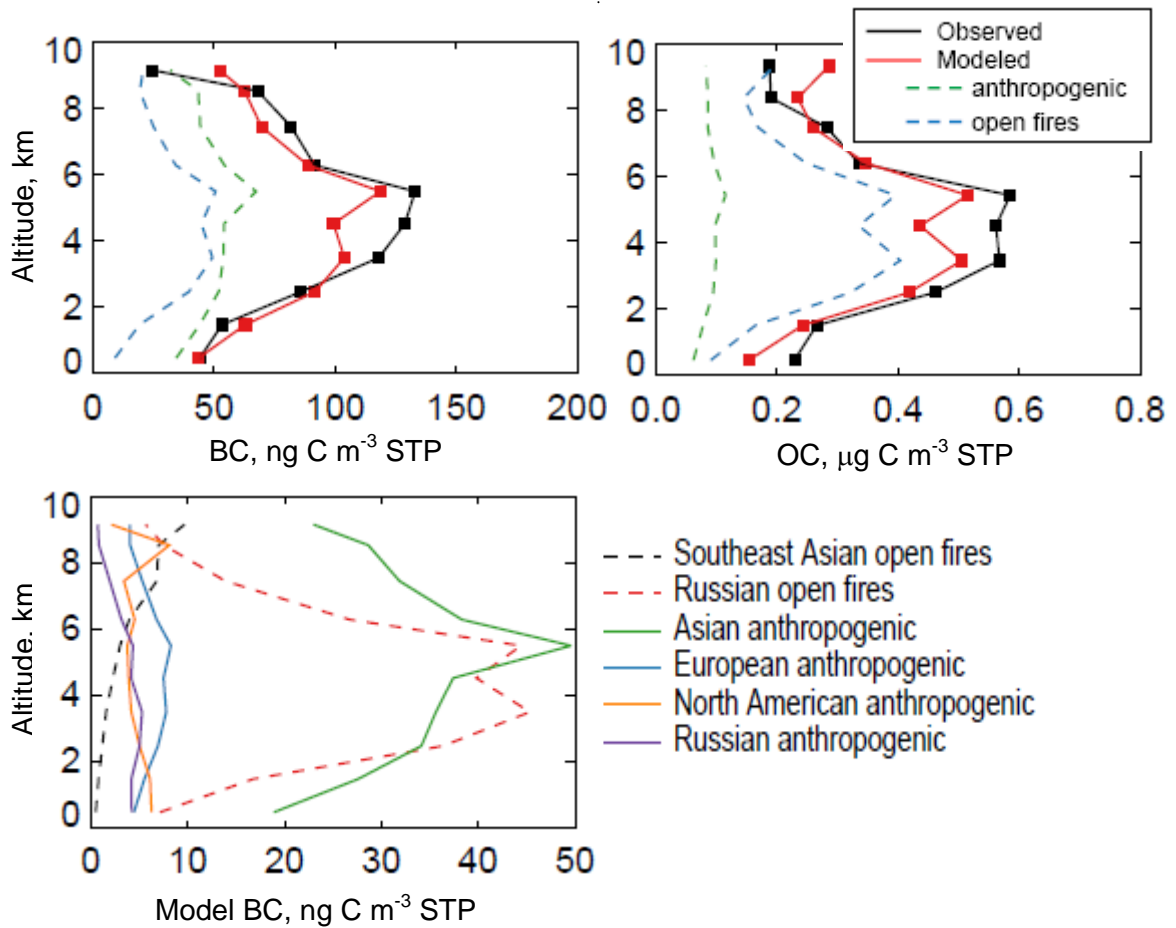


Fig. 7. Mean vertical profiles of BC and OA concentrations along the DC-8 flight tracks in ARCTAS (1-19 April 2008), averaged over 1-km altitude bins. The top panels compare observations to GEOS-Chem and separate the model contributions from anthropogenic and open fire sources. The bottom panel further separates model BC contributions by source regions. Anthropogenic sources include fossil fuel and biofuel combustion.

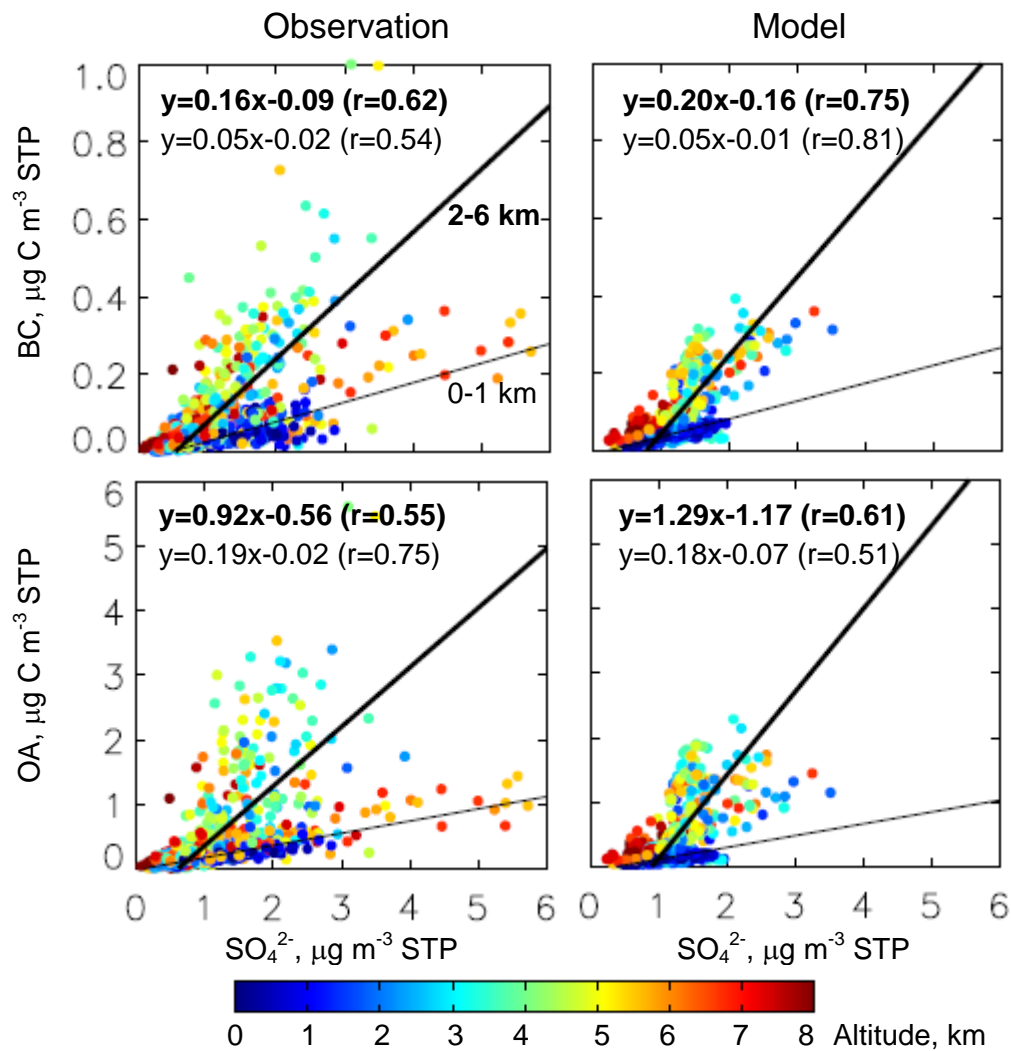


Fig. 8. Scatterplots of BC and OA vs. sulfate ( $\text{SO}_4^{2-}$ ) concentrations in ARCTAS. Observations from the DC-8 aircraft (left panels) are compared to model values sampled along the aircraft flight tracks (right panels). Individual points are colored by altitude. Reduced-major-axis (RMA) regression statistics and linear fits are shown in thin black for near-surface data (<1 km) and in thick black for mid-tropospheric data (2-6 km).

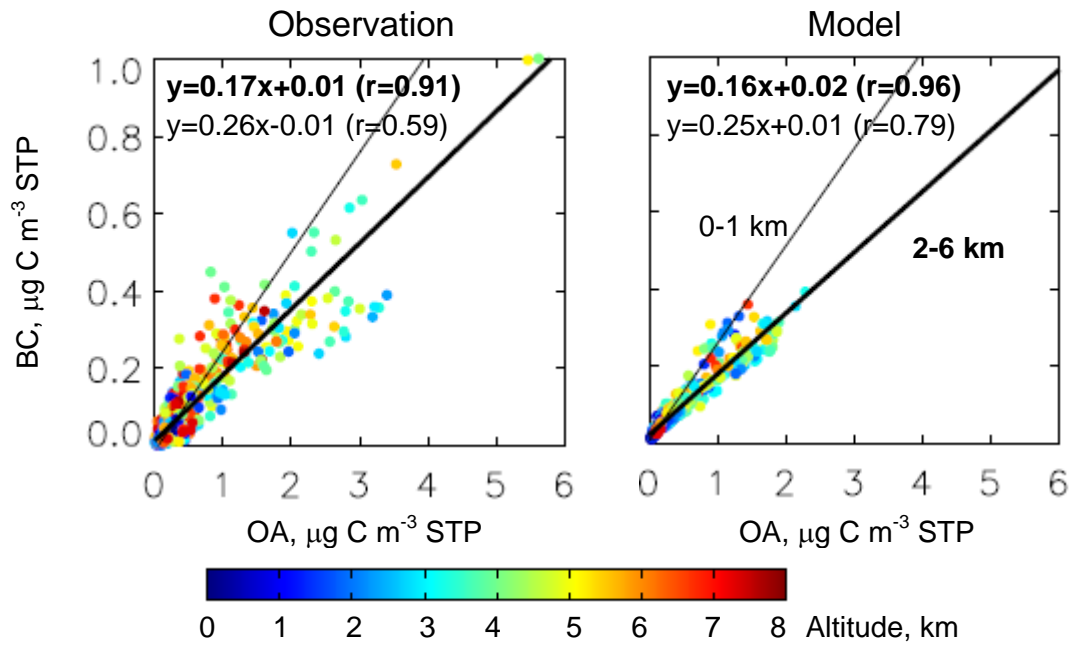


Fig. 9. Same as Fig. 8 but for BC vs. OA concentrations in ARCTAS.

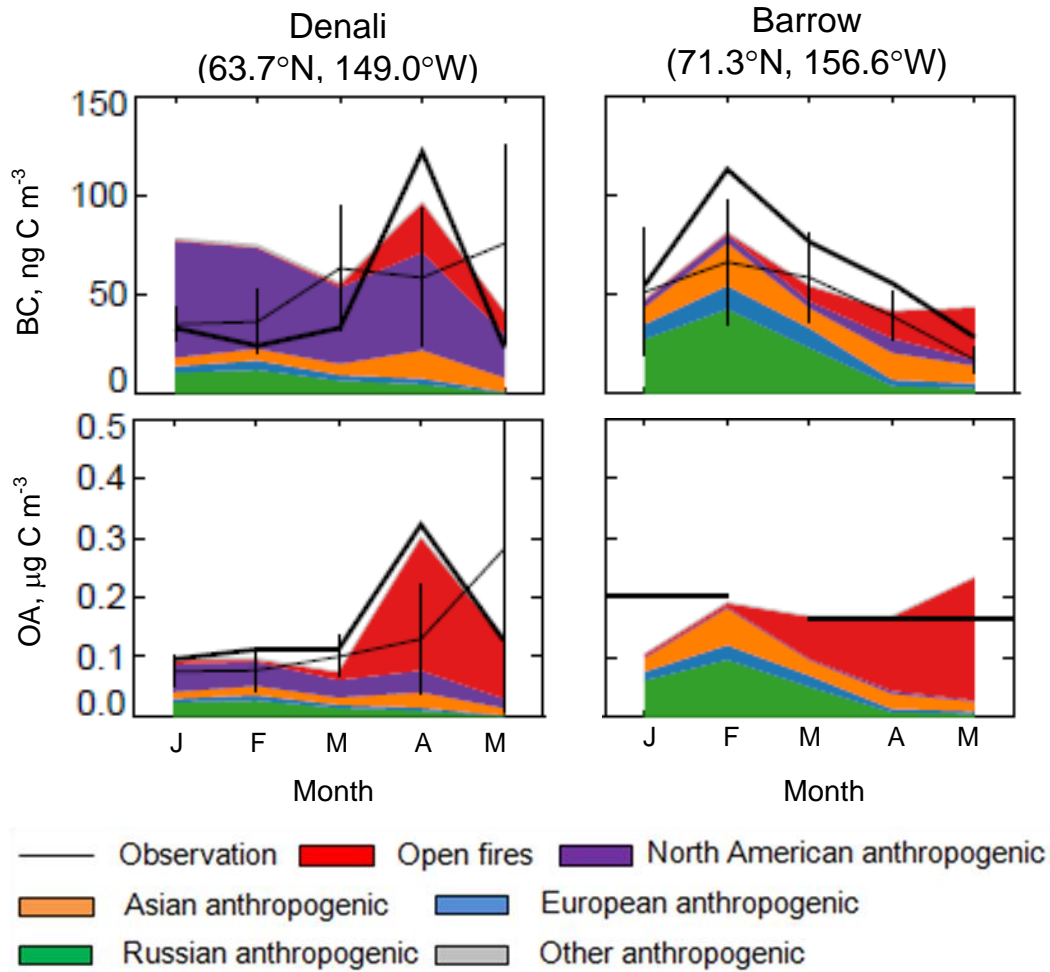


Fig. 10. Seasonal variation of BC and OA surface air concentrations at Denali and Barrow in Alaska. The thick black lines are monthly mean observations for 2008. The thin black lines are monthly mean observations for 2002-2008 with vertical bars representing interannual standard deviations. The thick line for OA at Barrow represents seasonal mean concentrations in Nov 2008-Feb 2009 and Mar-Jun 2008 from P. Shaw et al. (2010). Additive model contributions from different sources in the 2008 simulation are shown in color.

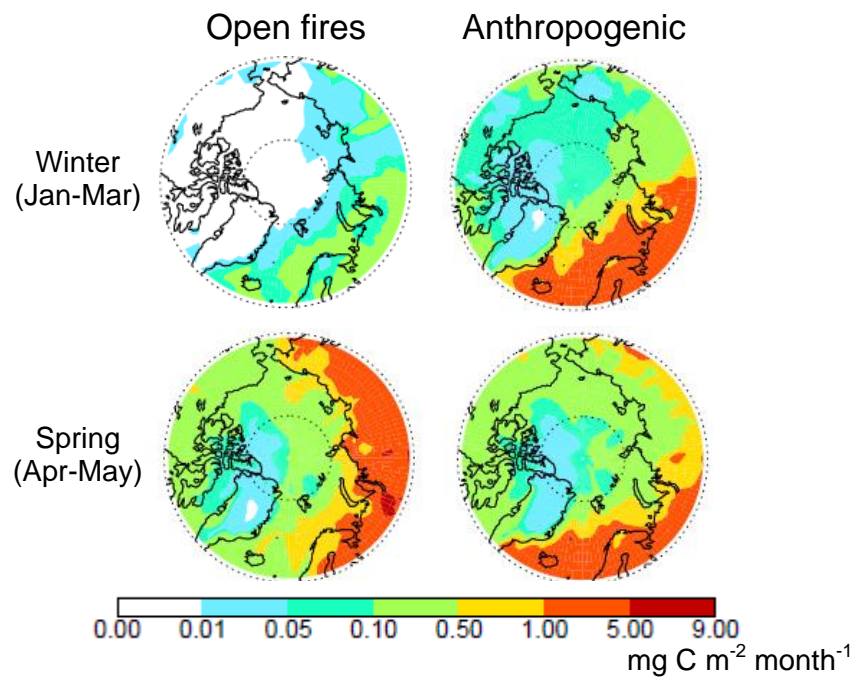


Fig. 11. Contributions of open fire and anthropogenic (fuel combustion) sources to the BC deposition flux in GEOS-Chem for winter and spring 2008.

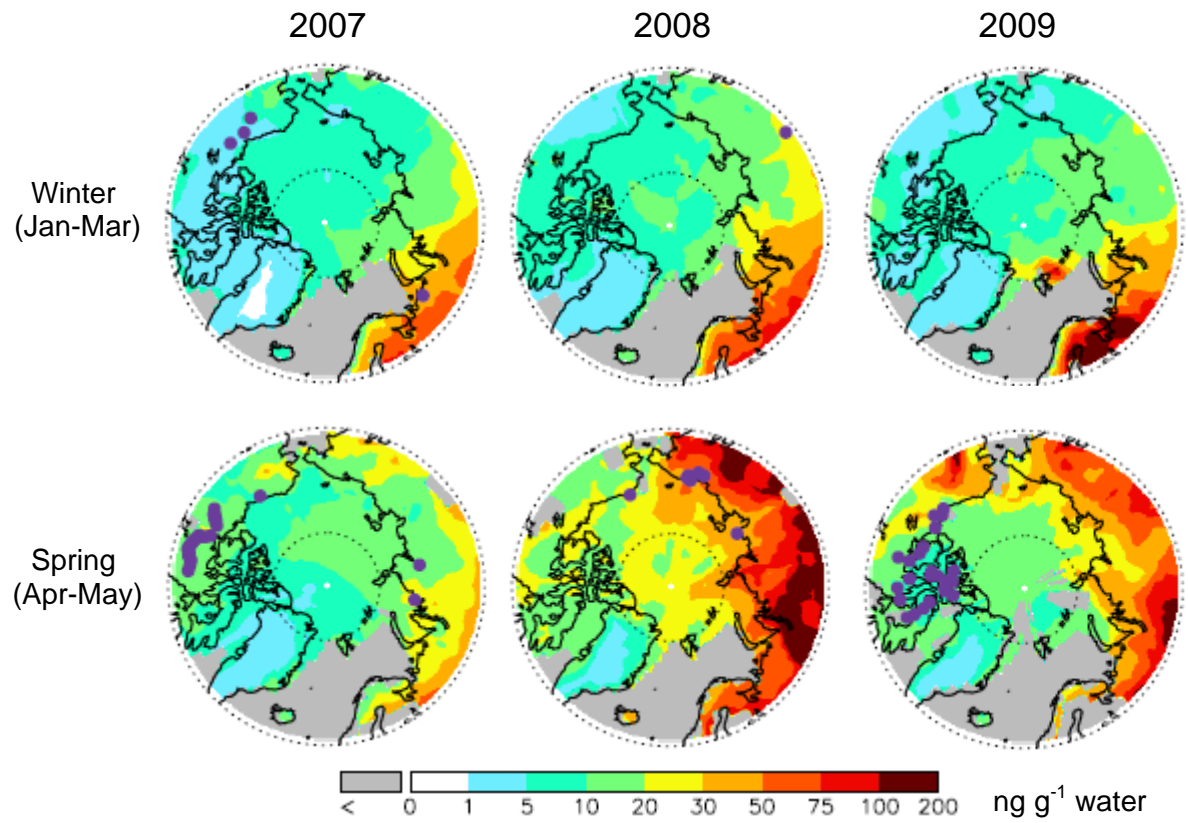


Fig. 12. Simulated BC content of Arctic snow in winter and spring 2007-2009. Snow-free areas are shown in gray. Purple circles indicate snow sampling sites from Doherty et al. (2010) for the corresponding years and seasons.

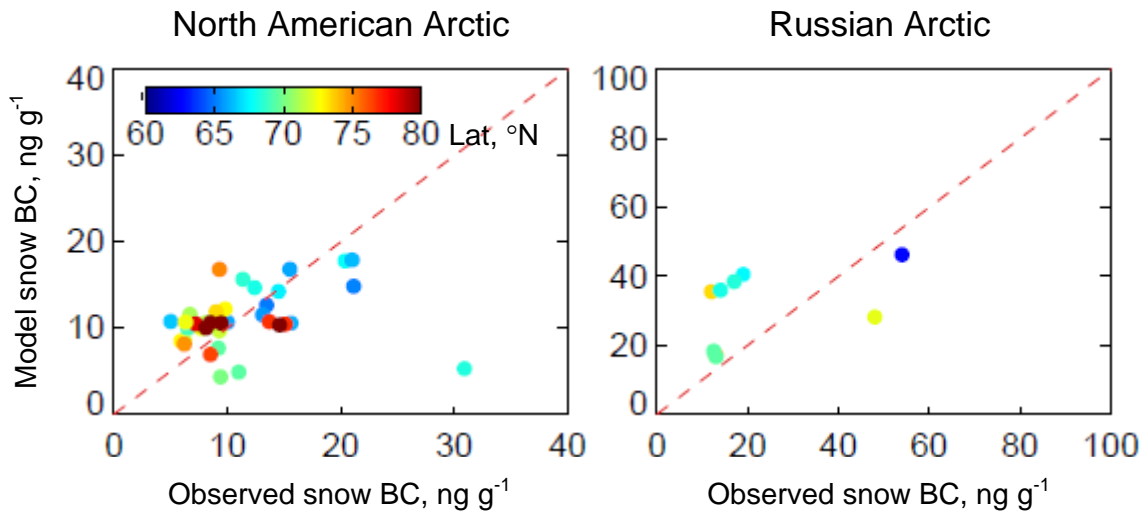


Fig. 13. Scatterplots of simulated vs. observed BC content in snow for North American and Russian Arctic sites in Mar-May 2007-2009 (Figure 12). Observations from Doherty et al. (2010) are averaged over model grid squares, and model results are sampled for the month and year of observations. The data are colored by latitude. Also shown is the 1:1 line.

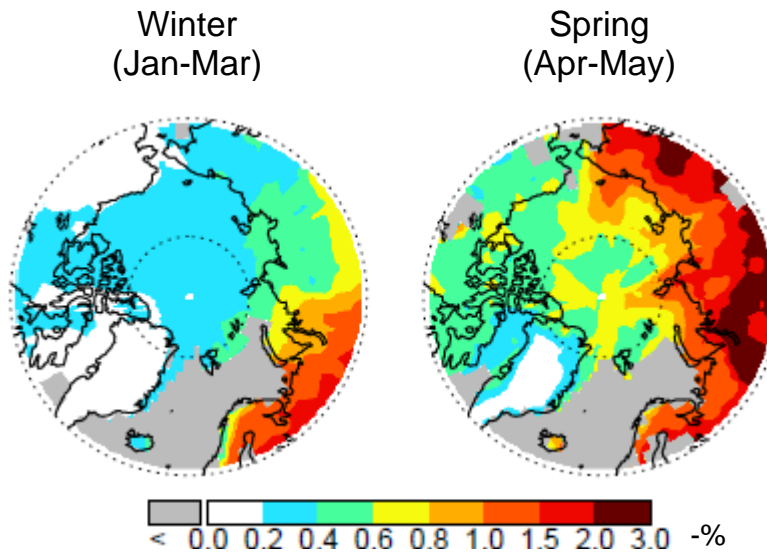


Fig. 14. Model decreases in snow albedo due to BC deposition in the Arctic ( $>60^{\circ}\text{N}$ ) in winter and spring 2008. Snow-free areas are shown in gray.